Using *Semtex*

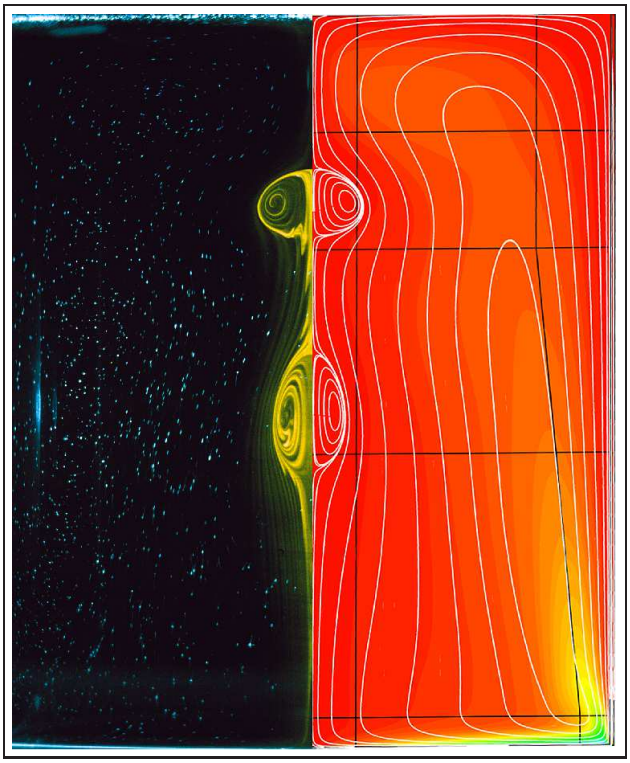

H. M. Blackburn
Monash University

October 6, 2017
Semtex version 8.2

Contents

Chapter 1

Introduction

Semtex is a family of spectral element simulation codes, most prominently a code for direct numerical simulation of incompressible flow. The spectral element method is a high-order finite element technique that combines the geometric flexibility of finite elements with the high accuracy of spectral methods. The method was pioneered in the mid 1980's by Anthony Patera at MIT (Patera; 1984; Korczak and Patera; 1986). *Semtex* uses parametrically mapped quadrilateral elements, the classic GLL 'nodal' shape function basis, and continuous Galerkin projection. Algorithmically the code is similar to Ron Henderson's *Prism* (Henderson and Karniadakis; 1995; Karniadakis and Henderson; 1998; Henderson; 1999), but with some differences in design, and lacks mortar element capability. A notable extension is that *Semtex* can solve problems in cylindrical as well as Cartesian coordinate systems (Blackburn and Sherwin; 2004).

1.1 Numerical method

Some central features of the spectral element method are

Orthogonal polynomial-based shape functions Spectral accuracy is achieved by using tensor-product Lagrange interpolants within each element, where the nodes of these shape functions are placed at the zeros of Legendre polynomials mapped from the canonical domain [-1, 1]×[-1, 1] to each element. In one spatial dimension, the resulting Gauss–Lobatto–Legendre Lagrange interpolant which is unity at one of the $N+1$ Gauss–Lobatto points x_j in [-1, 1] and zero at the others is

$$\psi_j(x) = \frac{1}{N(N+1)L_N(x_j)} \frac{(1-x^2)L'_N(x)}{x-x_j}. \tag{1.1}$$

For example, the family of sixth-order GLL Lagrange interpolants is shown in figure 1.1. In smooth function spaces it can be shown that the resulting interpolants converge exponentially

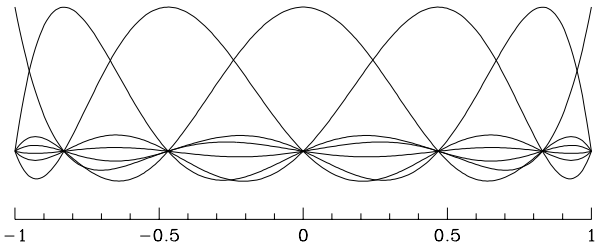

Figure 1.1: The family of sixth-order one-dimensional GLL Lagrange shape functions on the master domain $[-1, +1]$.

fast (faster than any negative integer power of N) as the order of the interpolant is increased. See Canuto et al. (1988), §§ 2.3.2 and 9.4.3.

Gauss–Lobatto quadrature Efficiency (particularly in iterative methods) is achieved by using Gauss–Lobatto quadrature for evaluating elemental integrals: the quadrature points reside at the nodal points, which enables fast tensor-product techniques to be used for iterative matrix solution methods. Gauss–Lobatto quadrature on the nodal points delivers diagonal mass matrices.

Static condensation Direct matrix solutions are sped up by using static condensation coupled with bandwidth reduction algorithms to reduce storage requirements for assembled system matrices.

While the numerical method is very accurate and efficient, it also has the advantage that complex geometries can be accommodated by employing unstructured meshes. The vertices of spectral elements meshes can be produced using finite-element mesh generation procedures, or any other method (for *Semtex*, only meshes with quadrilateral elements are accepted).

Time integration employs a backwards-time differencing scheme described by Karniadakis et al. (1991), more recently classified as a velocity-correction method by Guermond and Shen (2003). One can select first, second, or third-order time integration, but second order is usually a reasonable compromise, and is the default scheme. Equal-order interpolation is used for velocity and pressure (see Guermond et al.; 2006).

As of *Semtex* V8, the 'alternating skew symmetric' form (Zang; 1991) is the default for construction of nonlinear terms in the Navier–Stokes equations (faster and just as robust as full skew symmetric, which is still an option), and no dealiasing of product terms is carried out for either serial or parallel operations. As an aid to robust operation at high Reynolds numbers, 'spectral vanishing viscosity' (Xu and Pasquetti; 2004) can easily be enabled by setting appropriate control tokens. A significant additional novelty of *Semtex* V8 is the option of robust outflow boundary conditions (Dong et al.; 2014), which alleviate much of the numerical stability problem associated with inflows that occur at the outflow boundary.

1.2 Implementation

The top level of the code is written in C++, with calls to C and FORTRAN library routines, e.g. BLAS and LAPACK. The original implementation for two-dimensional Cartesian geometries was extended to three dimensions using Fourier expansion functions for spatially-periodic directions in Cartesian and cylindrical spaces. Concurrent execution is supported, using MPI as the basis for interprocessor communications, and the code has been ported to DEC, NEC, Fujitsu, Compaq, SGI, Apple and Linux multiprocessor machines. Basically it ought to work with little trouble on any contemporary UNIX system.

There are various code extensions that are not part of the base distribution. These include dynamic and non-dynamic LES (Blackburn and Schmidt; 2003), simple power-law type non-Newtonian rheologies (Rudman and Blackburn; 2006), scalar transport (Blackburn; 2001, 2002a), buoyancy via the Boussinesq approximation, accelerating frame of reference coupling for aeroelasticity (Blackburn and Henderson; 1996, 1999; Blackburn et al.; 2000; Blackburn; 2003), solution of steady-state flows via Newton–Raphson iteration (Blackburn; 2002b)

However, linear stability analysis (Blackburn; 2002b; Blackburn and Lopez; 2003a,b; Blackburn et al.; 2005; Sherwin and Blackburn; 2005; Elston et al.; 2006; Blackburn and Sherwin; 2007) and optimal transient growth analysis (Blackburn et al.; 2008) are released as an additional code base (called *Dog*), see the accompanying user guide called 'Working *Dog*'.

1.3 Further reading

The most comprehensive references on spectral methods in general are Gottlieb and Orszag (1977), Canuto et al. (1988, 2006). The first papers by Patera (1984) and Korczak and Patera (1986) provide a good introduction to spectral elements, although some aspects have changed with time and Maday and Patera (1989) is more up-to-date. The use of Fourier expansions to extend the method to three spatial dimensions is discussed by Amon and Patera (1989), Karniadakis (1989) and Karniadakis (1990). The use of spectral element techniques in cylindrical coordinates is dealt with in Blackburn and Sherwin (2004). The book by Funaro (1997) provides useful information and further references. Recent overviews and some applications appear in Karniadakis and Henderson (1998); Henderson (1999). The definitive reference is now the book by Karniadakis and Sherwin (2005), but you will also find the text by Deville, Fischer and Mund (2002) useful for alternative explanations and views. More recently, the book by Canuto et al. (2007) provides both theory and applications of spectral as well as spectral element methods in fluid dynamics.

Chapter 2

Starting out

It is assumed you're using some version of UNIX (which includes Mac OS X), and the current *Semtex* versions assume that your C++ compiler supports the standard libraries. Makefiles assume GNUmake (by now this is usually the standard supplied variant of `make`). *SuperMongo* and *Tecplot* would be nice to have but are not essential to get up and running, and VTK-based post processors such as *VisIt* or *ParaView* can alternatively be used for post-processing in place of *Tecplot*. All major executables have a `-h` command line option which provides a usage prompt.

Application programs/Makefiles can be found in top and upper-level directories:

`elliptic`	Solve elliptic (Laplace, Poisson, Helmholtz) problems.
`dns`	Solve time-varying incompressible Navier–Stokes problems, Cartesian/cylindrical.

2.1 Testing

Unpack the tar file, then run `make test`. This will copy header files to their correct places, compile and place the libraries, make two central utilities (`compare` and `enumerate`), then make the direct numerical simulation solver `dns` and run regression checks on its output for a number of test cases. If all goes well, this process will end with a number of tests reported as `passed`. In that case, go on and compile all the utilities, too (`cd utility; make all`).

2.1.1 Troubleshooting installation problems

If the above process didn't work, there are a number of possible things lacking on your system, e.g.:

1. GNU's `make`: it needs to be in your `path` somewhere. On most current UNIX systems, the system-supplied `make` *is* the GNU version. So now (as of 2010) this is assumed; you can easily check by running `make --version` and looking at the first line of output. If not, it may be installed as `gmake`. Otherwise you will need to get it installed. Alter the variable `MAKE` in `semtex/Makefile` so that it gets to the installed GNU `make`, if required.

2. The BLAS and LAPACK libraries — these may be in `/usr/lib` or `/usr/local/lib`: search for `libblas` and `liblapack`. On many systems, BLAS and LAPACK are vendor-supplied as part of some 'math kernel' library. NB: since quite heavy use is made of BLAS routine `dgemm`, it can be worthwhile finding BLAS versions in which this is well optimised, see § 3.7.

3. A standard C++ compiler, a C compiler, and a FORTRAN compiler that can deal with FORTRAN-77. Note that F90, F95 compilers now often supplant F77 compilers, and these can (and should) be substituted if available. GNU's standard FORTRAN compiler is now called `gfortran` and is part of the standard `gcc` compiler suite.

4. Either `yacc` or `bison`.

If you have all these things but there are still compilation problems, you have some work to do.

The first place to look is in the file `src/Makefile` which has the master set of compilation flags and directives for various operating systems. You my find your system here, or one that is similar. Even if this is not the case, you should pick up some clues about how to set up for compilation on a new system. As well, check the `README` file in the top directory. Of course, it is possible that the code is incompatible with some detail of your compilation system or has a bug, but it has had fairly extensive exercise on a number of UNIX systems by now.

If you are having problems, it's usually best to start small and work up. First try to make and install the `veclib` and `femlib` libraries, since they do not use C++ or the linker. Try `make libs` at the top level, then if this is still problematic go to the `veclib` directory, do `make clean; make; make install`. When that works, do the same in the `femlib` directory. Next move on and try a simple C++ compile and link, e.g. in the `utility` directory do `make calc` and try running `calc` (which is a little like the UNIX calculator utility `bc`, but uses *Semtex*'s function parser, and links `libfem.a`, the library produced in `femlib`): try say `1+1`. Next you should try compiling something that links to the BLAS and LAPACK, e.g. `compare`. Once this will compile, everything should.

2.2 Files

Semtex uses a base input file which describes the mesh, boundary conditions. We call this a `session` file and typically it has no root extension. It is written in a format patterned on HTML, which we have called FEML (for Finite Element Markup Language). There are a number of example session files in the mesh directory. Other files have standard extensions:

`session.num`	Global node numbers, produced by enumerate utility.
`session.fld`	Solution/field file. Binary format by default.
`session.rst`	Restart file. Read in to initialize solution if present.
`session.avg`	Averaged results. Read back in for continuation (over-written).
`session.his`	History point data.
`session.flx`	Time series of pressure and viscous forces integrated over the `wall` boundary group.
`session.mdl`	Time series of kinetic energies in the Fourier modes.
`session.par`	Used to define initial particle locations.
`session.trk`	Integrated particle locations.

When writing a new session file it is best to run `meshpr` (and/or `meshpr -c`) on it before trying to use it for simulations. `Meshpr` will catch most of the easier-to-make errors. You can also plot up the results using *SuperMongo* or other utility as a visual check.

2.3 Utilities

Source code for these is found in the `utility` directory. You will need to make most of these by hand (using the supplied `Makefile`, and `make all`). Here is a summary:

`addfield`	Add vorticity vector components, divergence, etc., to a field file.
`calc`	A simple calculator that calls `femlib`'s function parser. The default functions and `TOKENS` can be seen if you run `calc -h`.
`compare`	Generate restart files, compare solutions to a function.
`convert`	Convert field file formats (IEEE-big/little, ASCII).
`eneq`	Compute terms in the energy transport equation.
`enumerate`	Generate global node numbering, with RCM optimization.
`integral`	Obtain the 2D integral of fields over the domain area.
`interp`	Interpolate a field file onto a (2D) set of points.

`meshpr`	Generate 2D mesh locations for plotting or checking.
`noiz`	Add a random perturbation to a field file.
`probe`	Probe a field file at a set of 2D/3D points. Different interfaces to `probe` are obtained through the names `probeline` and `probeplane`: make these soft links by hand.
`project`	Convert a field file to a different order interpolation.
`rectmesh`	Generate a template session file for a rectangular domain.
`resubmit`	Shell utility for automatic job resubmission.
`rstress`	Postprocess to compute Reynolds stresses from a file of time-averaged variables.
`save`	Shell utility for automatic job resubmission.
`sem2tec`	Convert field files to Amtec *Tecplot* format. Note that by default, `sem2tec` interpolates the original GLL- mesh-based data onto a (isoparametrically mapped) uniform mesh for improved visual appearance. Sometimes it is useful to see the original data (and mesh); for this use the `-n 0` command-line argument to `sem2tec`.
`sem2vtk`	Convert field files to VTK format (*VisIt, ParaView*).
`transform`	Take Fourier, Legendre, modal basis transform of a field file. Invertible.
`wallmesh`	Extract the mesh nodes corresponding to surfaces with the `wall` group.

Chapter 3

Examples and hints

We will run through some examples to illustrate input files, utility routines, and the use of the solvers.

3.1 2D Taylor flow

Taylor flow is an analytical solution to the Navier–Stokes equations. In the x–y plane the solution is

$$u = -\cos(\pi x)\sin(\pi y)\exp(-2\pi^2\nu t), \tag{3.1}$$
$$v = +\sin(\pi x)\cos(\pi y)\exp(-2\pi^2\nu t), \tag{3.2}$$
$$p = -(\cos(2\pi x)+\cos(2\pi y))\exp(-4\pi^2\nu t)/4. \tag{3.3}$$

The solution is doubly periodic in space, with periodic length 2. As usual for Navier–Stokes solutions, the pressure can only be specified up to an arbitrary constant. An interesting feature of this solution is that the nonlinear and pressure gradient terms balance one another, leaving a diffusive decay of the initial condition — this property is occasionally useful for checking codes.

3.1.1 Session file

Below is the complete input or *session* file we will use; it has four elements, each of the same size, with 11 nodes along each edge. We will call this session file `taylor2` in the following.

```
#############################################################################
# 2D Taylor flow in the x--y plane has the exact solution
#
#       u = -cos(PI*x)*sin(PI*y)*exp(-2.0*PI*PI*KINVIS*t)
#       v =  sin(PI*x)*cos(PI*y)*exp(-2.0*PI*PI*KINVIS*t)
#       w =  0
#       p = -0.25*(cos(2.0*PI*x)+cos(2.0*PI*y))*exp(-4.0*PI*PI*KINVIS*t)
#
# Use periodic boundaries (no BCs).

<USER>
        u = -cos(PI*x)*sin(PI*y)*exp(-2.0*PI*PI*KINVIS*t)
        v =  sin(PI*x)*cos(PI*y)*exp(-2.0*PI*PI*KINVIS*t)
        p = -0.25*(cos(TWOPI*x)+cos(TWOPI*y))*exp(-4.0*PI*PI*KINVIS*t)
</USER>

<FIELDS>
        u v p
</FIELDS>

<TOKENS>
```

```
        N_TIME  = 2
        N_P     = 11
        N_STEP  = 20
        D_T     = 0.02
        Re      = 100.0
        KINVIS  = 1.0/Re
        TOL_REL = 1e-12
</TOKENS>

<NODES NUMBER=9>
        1       0.0       0.0       0.0
        2       1.0       0.0       0.0
        3       2.0       0.0       0.0
        4       0.0       1.0       0.0
        5       1.0       1.0       0.0
        6       2.0       1.0       0.0
        7       0.0       2.0       0.0
        8       1.0       2.0       0.0
        9       2.0       2.0       0.0
</NODES>

<ELEMENTS NUMBER=4>
        1 <Q> 1 2 5 4 </Q>
        2 <Q> 2 3 6 5 </Q>
        3 <Q> 4 5 8 7 </Q>
        4 <Q> 5 6 9 8 </Q>
</ELEMENTS>

<SURFACES NUMBER=4>
        1       1       1       <P>     3       3       </P>
        2       2       1       <P>     4       3       </P>
        3       2       2       <P>     1       4       </P>
        4       4       2       <P>     3       4       </P>
</SURFACES>
```

The first section of the file in this case contains comments; a line anywhere in the session file which starts with a # is considered to be a comment. Following that are a number of sections which are opened and closed with matching keywords in HTML style (e.g. <USER>–<\USER>). Keywords are not case sensitive. The complete list of keywords is: TOKENS, FIELDS, GROUPS, BCS, NODES, ELEMENTS, SURFACES, CURVES and USER. Depending on the problem being solved, some sections may not be needed, but the minimal set is: FIELDS, NODES, ELEMENTS and SURFACES. Anywhere there is likely to be a long list of inputs within the sections, the NUMBER of inputs is also required; this currently applies to GROUPS, BCS, NODES, ELEMENTS, SURFACES and CURVES. In each of these cases the numeric tag appears first for each input, which is free-format. The order in which the sections appear in the session file is irrelevant.

The USER section is ignored by the solvers, and is used instead by utilities — in this case it will be used by the compare utility both to generate the initial condition or *restart* file and to check the computed solution. This section declares the variables corresponding to the solution fields with the corresponding analytical solutions. The variables x, y, z and t can be used to represent the three spatial coordinates and time. Note that some constants such as PI and TWOPI are predefined, while others, like KINVIS, are set in the TOKENS section. Note also the use of predefined functions, accessed through an inbuilt function parser[1].

The FIELDS section declares the one-character names of solution fields. The names are significant: u, v and w are the three velocity components (we only use u and v here for a 2D solution and the w

[1]The built-in functions and predefined constants can be found by running calc -h.

component is always the direction of Fourier expansions), p is the pressure field. The field name c is also recognized as a scalar field for certain solvers, e.g. the elliptic solver.

In the TOKENS section, second-order accurate time integration is selected (N_TIME = 2) and the number of Lagrange knot points along the side of each element is set to 11 (N_P = 11), corresponding to the use of 10th-order polynomials, and giving two-dimensional elemental shape functions which are tensor-products of 10th-order Lagrange polynomials.[2] The code will integrate for 20 timesteps (N_STEP = 20) with a timestep of 0.02 (D_T = 0.002). The kinematic viscosity is set as the inverse of the Reynolds number (100): note the use of the function parser here. Finally the relative tolerance used as a stopping test in the PCG iteration used to solve the viscous substep on the first timestep is set as 1.0×10^{-12}.

The shape of the mesh is defined by the NODES and ELEMENTS sections. Here there are four elements, each obtained by connecting the corner nodes in a counterclockwise traverse. The x, y and z locations of the nodes are given, and the four numbers given for the nodes of each element are indices within the list of nodes.

In the final section (SURFACES), we describe how the edges of elements which define the boundary of the solution domain are dealt with. In this example, the solution domain is periodic and there are no boundary conditions to be applied, so the SURFACES section describes only periodic (P) connections between elements. For example, on the first line, side 1 of element 1 is declared to be periodic with side 3 of element 3 — side 1 runs between the first and second nodes, while side 3 runs between the third and fourth.

3.1.2 Running the codes

Assume we're in the dns directory of the distribution, that the enumerate, compare, meshpr and sem2tec utilities have been compiled, as well as the dns simulation code.

```
karman[16] cp ../mesh/taylor2 .
```

First we'll examine the mesh, using *SuperMongo* macros.

```
karman[17] meshpr taylor2 > taylor2.msh
karman[18] sm
Hello Hugh, please give me a command
: meshplot taylor2.msh 1
Read lines 1 to 1 from taylor2.msh
Read lines 2 to 485 from taylor2.msh
: meshnum
: meshbox
: quit
```

You should have seen a plot like that in figure 3.1. (Note: while you are building up the mesh parts of a session file, you can use meshpr -c to suppress some of the checking for matching element edges and curved boundaries that meshpr does by default.)

Next we will generate the global numbering schemes for the solution using enumerate to produce taylor2.num. The solution code would run enumerate automatically to generate taylor2.num if it were not present, but we will run it 'by hand' to highlight its existence and illustrate its use.

```
karman[19] enumerate taylor2 > taylor2.num
karman[20] head -20 taylor2.num
# FIELDS         :  uvp
# ---------------  ----------
# 1 NUMBER SETS  :         uvp
# NEL            :           4
# NP_MAX         :          11
```

[2] The minimum accepted value of N_P = 2, corresponding to (bi)linear shape functions. The practicable upper value is around 20.

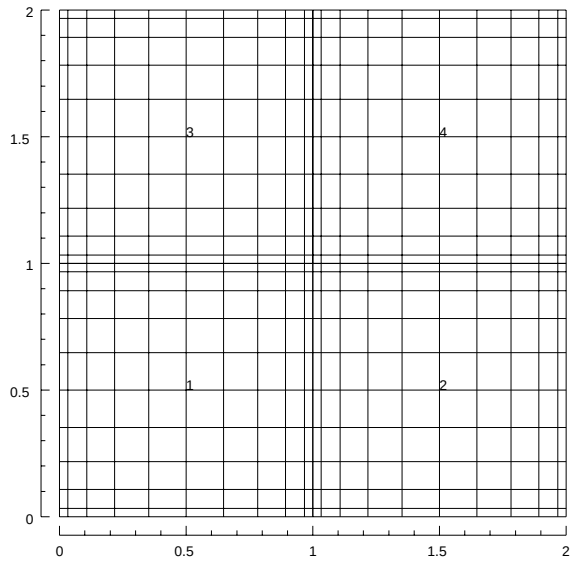

Figure 3.1: The mesh corresponding to the `taylor2` session file.

```
# NEXT_MAX       :          40
# NINT_MAX       :          81
# NTOTAL         :         484
# NBOUNDARY      :         160
# NGLOBAL        :          76
# NSOLVE         :          76
# OPTIMIZATION   :           1
# BANDWIDTH      :          67
# ---------------  ----------
# elmt  side offst  bmap  mask
     1     1     0    20     0
     1     1     1    17     0
     1     1     2    16     0
     1     1     3    15     0
     1     1     4    14     0
```

The `compare` utility is used to generate a file of initial conditions using information in the `USER` section of a session file. This *restart* file contains binary data, but we'll have a look at the start of it by converting it to ASCII format. Also, the header of these files is always in ASCII format, and so can be examined directly using the Unix `head` command.

```
karman[21] compare taylor2 > taylor2.rst
karman[22] convert taylor2.rst | head -20
taylor2                  Session
Wed Aug 13 21:39:47 1997  Created
11   11   1    4          Nr, Ns, Nz, Elements
0                        Step
0                        Time
0.02                     Time step
0.01                     Kinvis
1                        Beta
uvp                      Fields written
ASCII                    Format
     0.000000000      0.000000000    -0.5000000000
     0.000000000     0.1034847104    -0.4946454574
```

```
     0.000000000     0.3321033052    -0.4448536974
     0.000000000     0.6310660897    -0.3008777952
     0.000000000     0.8940117093    -0.1003715318
     0.000000000      1.000000000      0.000000000
     0.000000000     0.8940117093    -0.1003715318
     0.000000000     0.6310660897    -0.3008777952
     0.000000000     0.3321033052    -0.4448536974
     0.000000000     0.1034847104    -0.4946454574
```

Then the `dns` solver is run to generate a solution or *field* file, `taylor2.fld`. This has the same format as the restart file.

```
karman[23] dns taylor2
-- Restarting from file:  taylor2.rst
   Start time       : 0
   Time step        : 0.02
   Number of steps  : 20
   End time         : 0.4
   Integration order: 2
-- Building matrices for Fields "uvp"   [*]
-- Building matrices for Fields "uvp"   [.]
-- Building matrices for Fields "uvp"   [*]
Step: 1  Time: 0.02
Step: 2  Time: 0.04
Step: 3  Time: 0.06
Step: 4  Time: 0.08
Step: 5  Time: 0.1
Step: 6  Time: 0.12
Step: 7  Time: 0.14
Step: 8  Time: 0.16
Step: 9  Time: 0.18
Step: 10  Time: 0.2
Step: 11  Time: 0.22
Step: 12  Time: 0.24
Step: 13  Time: 0.26
Step: 14  Time: 0.28
Step: 15  Time: 0.3
Step: 16  Time: 0.32
Step: 17  Time: 0.34
Step: 18  Time: 0.36
Step: 19  Time: 0.38
Step: 20  Time: 0.4
```

We can use `compare` to examine how close the solution is to the analytical solution. The output of `compare` in this case is a field file which contains the difference: since we're only interested in seeing error norms here, we'll discard this field file.

```
karman[24] compare taylor2 taylor2.fld > /dev/null
Field 'u': norm_inf: 1.13019e-05
Field 'v': norm_inf: 1.13019e-05
Field 'p': norm_inf: 0.422391
```

The velocity error norms are small, as expected, but the pressure norm will always be arbitrary, corresponding to the fact that the pressure can only be specified to within an arbitrary constant.

Finally we will use `sem2tec` to generate a *Tecplot* input file. The *Tecplot* utility `preplot` must also be in your `path`.

```
karman[36] sem2tec -m taylor2.msh taylor2.fld
```

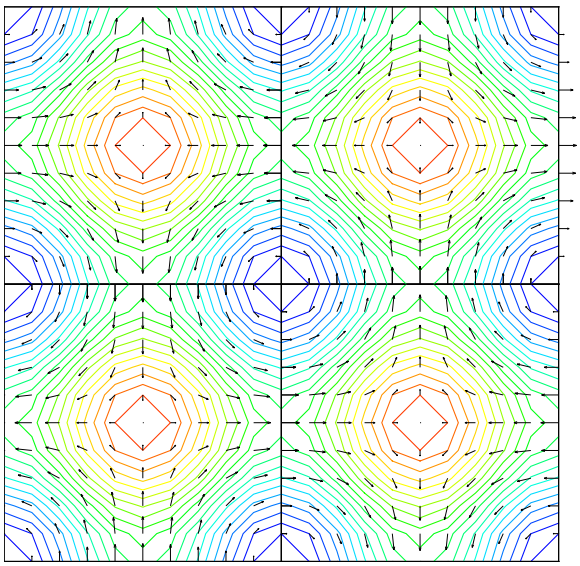

Figure 3.2: Solution to the `taylor2` problem, visualized using *Tecplot*.

This produces `taylor2.plt` which can be used as input to `tecplot`. The plot in figure 3.2 was generated using `tecplot` and shows pressure contours and velocity vectors. Notice that by default `sem2tec` interpolates the results from the Gauss–Lobatto–Legendre grid (seen in figure 3.1) used in the computation to a uniformly-spaced grid of the same order (use `-n 0` to disable this feature).

3.2 2D Laplace problem

In this section we illustrate the use of the elliptic solver for a 2D Laplace problem, $\nabla^2 c = 0$. In this case the function

$$c(x, y) = \sin(x) \exp(-y) \tag{3.4}$$

satisfies Laplace's equation and is used to set the boundary conditions. This example illustrates the methods used to set BCs and also to generate curved element boundaries. Also we will demonstrate the selection of the PCG solver. We will call the session file `laplace6`.

The elliptic solver can also be used to solve Poisson and Helmholtz problems in 2D and 3D Cartesian and cylindrical coordinate systems. Apart from this use it provides a means to test new formulations of elliptic solution routines used also in the Navier–Stokes type solvers.

```
#############################################################################
# Laplace problem on unit square, BC c(x, y) = sin(x)*exp(-y)
# is also the analytical solution.  Use essential (Dirichlet) BC
# on upper, curved edge, with natural (Neumann) BCs elsewhere.

<FIELDS>
        c
</FIELDS>

<USER>
        c =  sin(x)*exp(-y)
</USER>

<TOKENS>
        N_P      = 11
```

```
        TOL_REL  = 1e-12
        STEP_MAX = 1000
</TOKENS>

<GROUPS NUMBER=4>
        1       d       value
        2       a       slope
        3       b       slope
        4       c       slope
</GROUPS>

<BCS NUMBER=4>
        1       d       1
                        <D>     c =  sin(x)*exp(-y)     </D>
        2       a       1
                        <N>     c = -cos(x)*exp(-y)     </N>
        3       b       1
                        <N>     c =  cos(x)*exp(-y)     </N>
        4       c       1
                        <N>     c =  sin(x)*exp(-y)     </N>
</BCS>

<NODES NUMBER=9>
        1       0.0     0.0     0.0
        2       0.5     0.0     0.0
        3       1.0     0.0     0.0
        4       0.0     0.5     0.0
        5       0.5     0.5     0.0
        6       1.0     0.5     0.0
        7       0.0     1.0     0.0
        8       0.5     1.0     0.0
        9       1.0     1.0     0.0
</NODES>

<ELEMENTS NUMBER=4>
        1       <Q>     1 2 5 4         </Q>
        2       <Q>     2 3 6 5         </Q>
        3       <Q>     4 5 8 7         </Q>
        4       <Q>     5 6 9 8         </Q>
</ELEMENTS>

<SURFACES NUMBER=8>
        1       1       1       <B>     c       </B>
        2       2       1       <B>     c       </B>
        3       2       2       <B>     b       </B>
        4       4       2       <B>     b       </B>
        5       4       3       <B>     d       </B>
        6       3       3       <B>     d       </B>
        7       3       4       <B>     a       </B>
        8       1       4       <B>     a       </B>
</SURFACES>

<CURVES NUMBER=1>
        1       4       3       <ARC>   1.0     </ARC>
</CURVES>
```

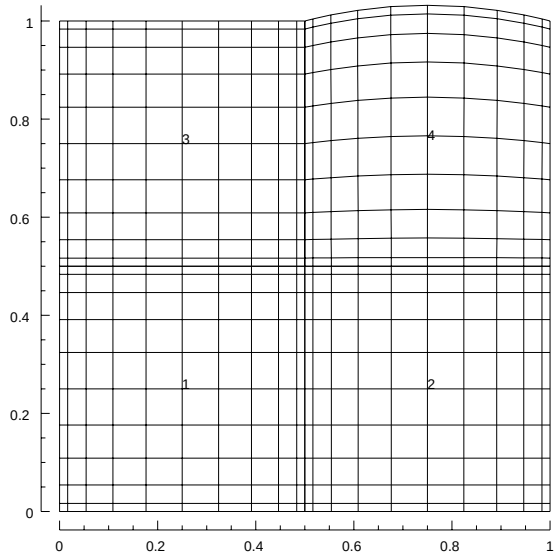

Figure 3.3: The mesh corresponding to the `laplace6` session file.

3.2.1 Curved element edges

The mesh is somewhat similar to that for the Taylor flow example, the only difference being in the use of a curved edge for the 3rd edge of element 4, as specified in the `CURVES` section. Both `ARC` and `SPLINE` type curves are currently implemented. For the `ARC` type, the parameter supplies the radius of the curve: a positive value implies that the curve makes the element convex on that side, while a negative value implies a concave side. Note that where elements mate along a curved side, the curve must be defined twice, once for each element, and with radii of different signs on each side. The mesh for this problem can be seen in figure 3.3.

For the `SPLINE` type, the parameter supplies the name of an ASCII file which contains a list of (x, y) coordinate pairs (white-space delimited). Naturally, the list of points should be in arc-length order. A single file can be used to supply the curved edges for a set of element edges. The vertices of the relevant elements do not have to lie exactly on the splined curve — if they do not, those vertices get shifted to the intersection of the projection of the straight line joining the original vertex position and its neighbouring "curve-normal' vertex, and the cubic spline joining the points in the file. On the other hand, it is good practise to ensure that the declared vertex locations lie close to the spline, and to check the mesh that is produced: use `meshpr` to do this.

3.2.2 Boundary conditions

The other new sections introduced in the session file for this example (`GROUPS`, `BCS`) are used to impose boundary conditions on the problem. The `GROUPS` section associates a character group tag (e.g. `d`) with a string (e.g. `value`), but note that different groups can be associated with the same string[3]. Groups `a`, `b` and `c` will be used to set natural (i.e. slope or Neumann), boundary conditions ($\partial c/\partial n = \text{value}$), while group `a` will be used to impose an essential or Dirichlet condition ($c = \text{value}$).

The `BCS` section is used to define the boundary conditions which will be applied for each group. For each group, after the numeric tag (ignored) appears the character for that group, then the number of BCs that will be applied: this corresponds to the number of fields in the problem, in this case 1 (`c`). BCs are typically of Dirichlet, Neumann, or mixed type (note that domain periodicity can be

[3]This allows actions to be taken over a set of BCs which share the same string.

employed but that this does not constitute a boundary condition). So in this case we will declare the BC types to be D (Dirichlet) for group d and N (Neumann) for groups a, b and c. On Neumann boundaries, the value which must be supplied is the slope of the solution along the outward normal to the solution domain. Note the fact that the BCs can be set using the function parser, using the built-in functions and variables, also any symbols defined in the TOKENS section, as well as the spatial variables x, y and z. The BCs can also be functions of time, t, and for time-varying problems the boundary conditions are re-evaluated every time step.

The BC groups are associated with element edges in the SURFACES section, in a similar way to the use of periodic boundaries for the taylor2 problem, although the edges are set to be B (BC) rather than P (periodic).

Periodic edges, Dirichlet, Neumann and mixed boundary conditions can be arbitrarily combined in a problem. Dirichlet conditions over-ride Neumann ones where they meet (say at the corner node of an element). See further discussion on boundary conditions in § 3.5 below.

3.2.3 Running the codes

We will run the solver and compare the computed solution to the analytical solution. We will select the iterative (PCG) solver using the -i command-line option to elliptic, then check the result using compare.

```
karman[287] elliptic -i laplace6
-- Initializing solution with zero IC
   Start time       : 0
   Time step        : 0.01
   Number of steps  : 1
   End time         : 0.01
   Integration order: 2
karman[288] compare laplace6 laplace6.fld > /dev/null
Field 'c': norm_inf: 1.37112e-08
```

Next try the direct solver (default):

```
karman[288] compare laplace6 laplace6.fld > /dev/null
Field 'c': norm_inf: 1.37112e-08
karman[289] elliptic laplace6
-- Initializing solution with zero IC
   Start time       : 0
   Time step        : 0.01
   Number of steps  : 1
   End time         : 0.01
   Integration order: 2
-- Building matrices for Fields "c"     [*]
karman[290] compare laplace6 laplace6.fld > /dev/null
Field 'c': norm_inf: 3.10862e-15
```

In this case the direct solver is more accurate, but comparable accuracy with the iterative solver could be obtained by decreasing TOL_REL in the TOKENS section (and further increasing STEP_MAX, which has a default value of 500).

3.3 3D Kovasznay flow

Here we will solve another viscous flow for which an analytical solution exists, the Kovasznay flow (we will call the session file `kovas3`). In the x–y plane, this flow is

$$u = 1 - \exp(\lambda x)\cos(2\pi y) \tag{3.5}$$
$$v = \lambda/(2\pi)\exp(\lambda x)\sin(2\pi y) \tag{3.6}$$
$$w = 0 \tag{3.7}$$
$$p = (1 - \exp(\lambda x))/2 \tag{3.8}$$

where $\lambda = Re/2 - (0.25Re^2 + 4\pi^2)^{1/2}$.

Although the solution has only two velocity components, we will set up and solve the problem in three dimensions, with a periodic length in the z direction of 1.0 and 8 z planes of data. The length in the z direction is set within the code by the variable `BETA` where $\beta = 2\pi/L_z$. The default value of `BETA` is 1, so we reset this in the `TOKENS` section using the function parser. The exact velocity boundary conditions are supplied on at the left and right edges of the domain, and periodic boundaries are used on the upper and lower edges (the domain has $-0.5 \leq y \leq 0.5$). Since the flow evolves to a steady state, first order timestepping is employed (`N_TIME = 1`).

```
###############################################################################
# Kovasznay flow in the x--y plane has the exact solution
#
#       u = 1 - exp(lambda*x)*cos(2*PI*y)
#       v = lambda/(2*PI)*exp(lambda*x)*sin(2*PI*y)
#       w = 0
#       p = (1 - exp(lambda*x))/2
#
# where lambda = Re/2 - sqrt(0.25*Re*Re + 4*PI*PI).
#
# This 3D version uses symmetry planes on the upper and lower boundaries
# with flow in the x-y plane.
#
# Solution accuracy is independent of N_Z since all flow is in the x--y plane.

<USER>
        u = 1.0-exp(LAMBDA*x)*cos(TWOPI*y)
        v = LAMBDA/(TWOPI)*exp(LAMBDA*x)*sin(TWOPI*y)
        w = 0.0
        p = 0.5*(1.0-exp(LAMBDA*x))
</USER>

<FIELDS>
        u v w p
</FIELDS>

<TOKENS>
        N_Z    = 8
        N_TIME = 1
        N_P    = 8
        N_STEP = 500
        D_T    = 0.008
        Re     = 40.0
        KINVIS = 1.0/Re
        LAMBDA = Re/2.0-sqrt(0.25*Re*Re+4.0*PI*PI)
        Lz     = 1.0
        BETA   = TWOPI/Lz
```

```
</TOKENS>

<GROUPS NUMBER=1>
        1       v       velocity
</GROUPS>

<BCS NUMBER=1>
        1       v       4
                        <D> u = 1-exp(LAMBDA*x)*cos(2*PI*y)             </D>
                        <D> v = LAMBDA/(2*PI)*exp(LAMBDA*x)*sin(2*PI*y) </D>
                        <D> w = 0.0                                     </D>
                        <H> p                                           </H>
</BCS>

<NODES NUMBER=9>
        1      -0.5    -0.5     0.0
        2       0      -0.5     0.0
        3       1      -0.5     0.0
        4      -0.5     0       0.0
        5       0       0       0.0
        6       1       0       0.0
        7      -0.5     0.5     0.0
        8       0       0.5     0.0
        9       1       0.5     0.0
</NODES>

<ELEMENTS NUMBER=4>
        1 <Q> 1 2 5 4 </Q>
        2 <Q> 2 3 6 5 </Q>
        3 <Q> 4 5 8 7 </Q>
        4 <Q> 5 6 9 8 </Q>
</ELEMENTS>

<SURFACES NUMBER=6>
        1       1       1       <P>     3       3       </P>
        2       2       1       <P>     4       3       </P>
        3       2       2       <B>     v               </B>
        4       4       2       <B>     v               </B>
        5       3       4       <B>     v               </B>
        6       1       4       <B>     v               </B>
</SURFACES>
```

3.3.1 'High-order' pressure boundary condition

Note that there is only one boundary group, and four boundary conditions must be set, corresponding to the four fields `u`, `v`, `w` and `p`. A new feature is a pressure BC of type `H`, which is an internally-computed Neumann boundary condition, (a High-order pressure BC) as described in Karniadakis et al. (1991). This is the kind of pressure BC that is supplied at all places except on outflow boundaries. The pressure BC is computed internally, so no value is required (if given, it will be ignored).

3.3.2 Running the codes

After running `dns`, we confirm there is only a single dump in the field file `kovas3.fld`, then run compare in order to examine the error norms for the solution. Following that we prepare input for *Tecplot*, projecting the interpolation to a 20×20 grid in each element. A view of the result can be seen in figure 3.4.

```
karman[25] convert kovas3.fld | grep -i session
```

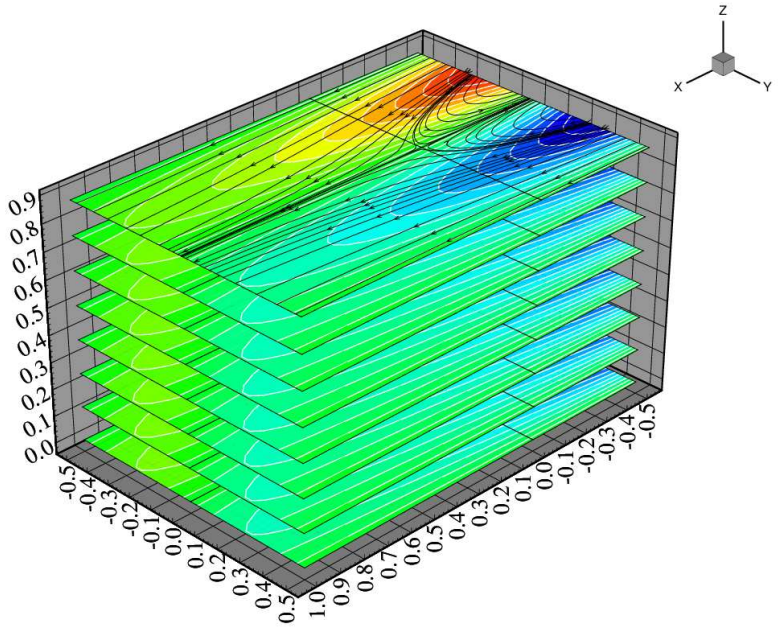

Figure 3.4: Solution to the `kovas3` problem, visualized using *Tecplot*. The plot shows contours of v velocity component and streamlines.

```
kovas3                    Session
karman[26] compare kovas3 kovas3.fld > /dev/null
Field 'u': norm_inf: 5.70744e-05
Field 'v': norm_inf: 3.04095e-05
Field 'w': norm_inf: 0
Field 'p': norm_inf: 0.928545
karman[27] meshpr kovas3 | sem2tec -n20 kovas3.fld
```

3.4 Vortex breakdown — a cylindrical-coordinate problem

Here we will examine a problem which uses the cylindrical coordinate option of `dns`. The physical situation is a cylindrical cavity, $H/R = 2.5$ with the flow driven by a spinning lid at one end. At the Reynolds number we'll use, $Re = \Omega R^2/\nu = 2119$, a vortex breakdown is known to occur. The flow in this case is invariant in the azimuthal direction, but has three velocity components (it is 2D/3C). In the cylindrical code, the order of spatial directions and velocity components is z, r, θ.

Note that for a full circle in the azimuthal direction, `BETA = 1.0`, (which is the default value). In fact, the value would not be used in the present solution, since all derivatives in the azimuthal direction are implicitly zero when `N_Z=1`. (But see § 3.4.1 below.)

```
#############################################################################
# 15 element driven cavity flow.

<FIELDS>
        u v w p
</FIELDS>

<TOKENS>
        CYLINDRICAL = 1
        N_Z         = 1
        BETA        = 1.0
```

```
        N_TIME      = 2
        N_P         = 11
        N_STEP      = 100000
        D_T         = 0.01
Re          = 2119
        KINVIS      = 1/Re
        OMEGA       = 1.0
        TOL_REL     = 1e-12
</TOKENS>

<GROUPS NUMBER=3>
        1       v       velocity
        2       w       wall
        3       a       axis
</GROUPS>

<BCS NUMBER=3>
        1       v       4
                        <D>     u = 0           </D>
                        <D>     v = 0           </D>
                        <D>     w = OMEGA*y     </D>
                        <H>     p               </H>
        2       w       4
                        <D>     u = 0           </D>
                        <D>     v = 0           </D>
                        <D>     w = 0           </D>
                        <H>     p               </H>
        3       a       4
                        <A>     u               </A>
                        <A>     v               </A>
                        <A>     w               </A>
                        <A>     p               </A>
</BCS>

<NODES NUMBER=24>
        1       0       0       0
        2       0.4     0       0
        3       0.8     0       0
        4       1.5     0       0
        5       2.4     0       0
        6       2.5     0       0
        7       0       0.15    0
        8       0.4     0.15    0
        9       0.8     0.15    0
        10      1.5     0.15    0
        11      2.4     0.15    0
        12      2.5     0.15    0
        13      0       0.75    0
        14      0.4     0.75    0
        15      0.8     0.75    0
        16      1.5     0.818   0
        17      2.4     0.9     0
        18      2.5     0.9     0
        19      0       1       0
        20      0.4     1       0
        21      0.8     1       0
        22      1.5     1       0
        23      2.4     1       0
```

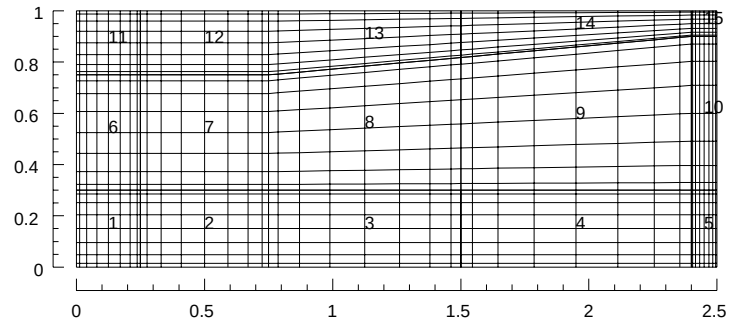

Figure 3.5: Mesh for the vortex breakdown problem. The spinning lid is at right.

```
        24      2.5     1       0
</NODES>

<ELEMENTS NUMBER=15>
        1       <Q>      1  2  8  7     </Q>
        2       <Q>      2  3  9  8     </Q>
        3       <Q>      3  4 10  9     </Q>
        4       <Q>      4  5 11 10     </Q>
        5       <Q>      5  6 12 11     </Q>
        6       <Q>      7  8 14 13     </Q>
        7       <Q>      8  9 15 14     </Q>
        8       <Q>      9 10 16 15     </Q>
        9       <Q>     10 11 17 16     </Q>
        10      <Q>     11 12 18 17     </Q>
        11      <Q>     13 14 20 19     </Q>
        12      <Q>     14 15 21 20     </Q>
        13      <Q>     15 16 22 21     </Q>
        14      <Q>     16 17 23 22     </Q>
        15      <Q>     17 18 24 23     </Q>
</ELEMENTS>

<SURFACES NUMBER=16>
        1       1       1       <B>     a       </B>
        2       2       1       <B>     a       </B>
        3       3       1       <B>     a       </B>
        4       4       1       <B>     a       </B>
        5       5       1       <B>     a       </B>
        6       5       2       <B>     v       </B>
        7       10      2       <B>     v       </B>
        8       15      2       <B>     v       </B>
        9       15      3       <B>     w       </B>
        10      14      3       <B>     w       </B>
        11      13      3       <B>     w       </B>
        12      12      3       <B>     w       </B>
        13      11      3       <B>     w       </B>
        14      11      4       <B>     w       </B>
        15      6       4       <B>     w       </B>
        16      1       4       <B>     w       </B>
</SURFACES>
```

The mesh for the problem is shown in figure 3.5, and the velocity field is shown compared to an experimental streakline flow visualisation on the front cover of this document.

3.4.1 BCs for cylindrical coordinates

A new feature here is the use of BCs of type `A` on the axis of the flow. Internally, the code sets the BC there either as zero essential or zero natural, depending on the physical variable and the Fourier mode. Owing to the coupling scheme used in the code (Blackburn and Sherwin; 2004), the boundary conditions for the radial and azimuthal velocities `v` and `w` must be of the same type within each group. A further restriction is that the group to which the axis belongs must have name `axis`.

Finally, say you wish to solve a cylindrical-coordinate problem where you know there is an n-fold azimuthal symmetry (say $n = 3$). In that case, it is much cheaper to solve with `BETA=3`, and use one-third the number of azimuthal planes that would be required for `BETA=1`.

3.5 Boundary condition roundup

The basic types of boundary conditions the code can deal with are Dirichlet type (value of variable is set, a.k.a. an *essential* boundary condition in the finite element community) and Neumann type (boundary-normal gradient of value is approximated, a.k.a. a *natural* type boundary condition in the finite-element community). The code can also deal with boundary conditions of mixed type (a linear combination of Dirichlet and Neumann). We note that periodic domain boundary surfaces (`<P>`) are allowed, but strictly speaking, periodicity does not constitute a boundary condition as such. Also we remark that for our code(s), boundary conditions may only be set for variables involved in elliptic sub-problems where, owing to the MWR treatment, Neumann boundary conditions are implemented as integral approximations (which converge to the given value pointwise as resolution is increased), while Dirichlet conditions are 'lifted' out of the problem and imposed exactly to the values which are set by the user.

Standard Dirichlet and Neumann boundary conditions may be supplied as a string that can be parsed by the solver to obtain a real value, based on predefined and user-declared `TOKENS`, and also the space/time variables `x`, `y`, `z` and `t`. These strings are re-parsed at each time step, so time-varying boundary conditions are allowed. We have already seen examples of these BC declarations in §§ 3.2, 3.3 and 3.4. Note that the strings involved should not contain white space.

We have not yet described mixed boundary conditions. These are of type $\partial c/\partial n + K(c - C) = 0$ where C and K are constants. Here, n signifies the unit outward normal direction: $\partial c/\partial n = \boldsymbol{n} \cdot \boldsymbol{\nabla} \boldsymbol{c}$. Mixed boundary conditions are specified in the form `<M> field = mulval;refval </M>` where `mulval` is (a string that evaluates to) the real value K and `refval` is (a string that evaluates to) the real value C. At present for mixed BCs, unlike Dirichlet and Neumann boundary conditions, C and K are fixed at the values they initially evaluate to (not time-varying).

In Navier–Stokes type problems, various of the above boundary conditions for the velocity and pressure variables are typically combined in set ways. In some cases, the user does not provide values or choose the combination since the boundary conditions are computed internally. Below we supply as examples various typical boundary condition sets which would be located in the `BCS` section of a session file. As written, they are for two-component Navier–Stokes problems but the generalisation to three-component problems should be obvious.

See also § 3.2 of the *Dog* user guide for a discussion of sets of boundary condtions appropriate for symmetry and anti-symmetry boundaries.

3.5.1 No-slip wall

```
<D> u = 0.0 </D>
<D> v = 0.0 </D>
<H> p       </H>
```

The tag `H` for pressure (`p`) denotes an internally computed 'high-order' Neumann condition, as originally described by Karniadakis et al. (1991). If the associated `GROUP` string is `wall` then tractions

will contribute to the integrated values found in `session.flx` file, see § 4.4.

3.5.2 Inflow or prescribed-velocity boundary

```
<D> u = 1.0 </D>
<D> v = 0.0 </D>
<H> p       </H>
```

Note that either of the supplied values can be a string to be evaluated by the parser at each timestep.

3.5.3 Slip (no-penetration) boundary

```
<N> u = 0.0 </N>
<D> v = 0.0 </D>
<H> p       </H>
```

Note that in this case, the boundary needs to be aligned with the x axis. At present there is no way to set a slip boundary which is inclined or curved; it must be parallel to either the x or y axis.

3.5.4 'Stress-free' outflow boundary

```
<N> u = 0.0 </N>
<N> v = 0.0 </N>
<D> p = 0.0 </D>
```

This is a restricted approximation to a true stress-free boundary where the tractions are zero. This boundary is also stress-free but achieves the condition by ensuring that the viscous and pressure tractions are individually zero, rather than their sum.

3.5.5 'Robust' outflow boundary

```
<O> u </O>
<O> v </O>
<O> p </O>
```

This is a set of computed boundary conditions (computed Neumann for velocity and computed Dirichlet for pressure). (In fact if `w` is included, its boundary condition is set as $\partial w/\partial n = 0$ rather than being computed.) This boundary condition was originally described in Dong et al. (2014), and is based on maintaining boundedness of kinetic energy within the domain. It is excellent for maintaining stability for flows in short open domains, where the use of the 'stress-free' condition described in § 3.5.4 can lead to catastrophe if significant inflow occurs over an outflow boundary. Type `O` boundaries must set the string `outflow` in their associated `GROUP`. In addition one must set the token `UODelta` (see eq. 4 of Dong et al.; 2014, this is $U_o\delta$) which is typically of order 0.1 or less.

3.5.6 Axis boundary

```
<A> u </A>
<A> v </A>
<A> p </A>
```

This is a set of Fourier-mode dependent homogeneous Dirichlet and Neumann boundary conditions to be used when the boundary coincides with the x axis of a cylindrical coordinate system as described in Blackburn and Sherwin (2004). Type `A` boundaries must set the string `axis` in their associated `GROUP`.

3.6 Fixing problems

You are liable to come up against a few generic problems when making and running your own cases. Here we will restrict discussion to Navier–Stokes problems and `dns`. The best diagnostic of trouble is the divergence of the solution. The code will output an estimate of the CFL-timestep every `IO_CFL` timesteps (default 50), along with the average divergence of the solution (in the operator-splitting used, incompressibility is only ensured in the spatial-convergence limit). Unfortunately the CFL estimate is presently unreliable, but the divergence energy provides an excellent diagnostic of trouble! If velocity and length scales are of order unity, the reported divergence energy should be much less than unity; if the divergence is large then either the solution is blowing up[4], or the spatial resolution is inadequate, or both.

By far the most common problem is that the solution will have a CFL-type instability brought about by using too large a time-step; this instability is unavoidably associated with using explicit time integration for the advection terms in the Navier–Stokes equations. This problem is easily enough fixed: try reducing `D_T` and increasing `N_STEP` to maintain the same integration interval. Obviously you will typically want `D_T` as large as possible, so if the problem runs stably, increase the timestep as much as is reasonable. If the velocity and timescales are of order unity, then the maximum timestep would typically be of order two orders of magnitude smaller (`0.01`). Note that CFL-stability will decrease with increasing time-integration order (`N_TIME`).

If the solution persists in blowing up when the timestep is reduced, the next most common cause is that there is inflow across an outflow boundary (in which case the problem is ill-posed, however, in practice *some* inflow across an outflow boundary over restricted times may be present without causing difficulty). To check if this is the cause, you could put some history points near the outflow (see § 4.7), but the best method of diagnosis is to run the solution up to a time when divergence starts to increase markedly, then use *Tecplot* or some other postprocessor to examine the solution near the outflow. This problem has been largely circumvented in *Semtex* V8 using the robust outflow BC set described by Dong et al. (2014), see § 3.5.5 above, though it cannot overcome all problems (e.g. an 'outflow' boundary with completely dominant inflow). In pathological cases of this sort, fixing the problem will generally require the mesh to be altered: sometimes the mesh is badly structured near the outflow (e.g. element sizes have been varied too rapidly); sometimes the problem can be overcome by extending the domain downstream; sometimes the domain needs to be reshaped (e.g. by contracting it in the cross-flow direction) so that there will be no outflow over the inflow boundary. If all else fails, consider the methods of § 4.12.3 to force the velocity near the outflow to be something more computationally tractable (if unphysical).

Any time you change the element polynomial order by changing `N_P`, or alter the structure of the boundary conditions, you should remake the numbering file `session.num`. It is especially important to remember this if you have changed the structure of the boundary conditions without changing element order, as no warning will be triggered; however, in this case you may no longer be actually applying the boundary conditions you have set in the session file because the `mask` values in `session.num` (which are set to `1` along a Dirichlet-type boundary) may no longer match what is implied by `session`.

3.7 Execution speed

Semtex relies heavily on the BLAS, so it can be worth seeking fast implementations. Especially, performance of matrix–matrix multiplication routine `dgemm` is critical. Consistently of late, Kazushige Goto's implementation of the BLAS gives best performance and is worth seeking out, although I understand his `dgemm` has also now been licenced to various vendors (Intel, AMD, Apple, ...) and is what you'll get if you link their extended math libraries.

[4] One wag suggested the name *Semtex* was associated with this property of the solutions.

As Reynolds numbers increase (i.e. `KINVIS` decreases), the viscous Helmholtz matrices in the operator splitting become more diagonally dominant and better conditioned. In this case, you may find that iterative (PCG) solution of the viscous step (obtained by setting `ITERATIVE=1` or running `dns -i`) is actually faster than the direct solution that is obtained by default. This is nice because additionally, less memory is required. It is generally worth checking this if you plan an extended series of runs, and Reynolds numbers are large.

Chapter 4

Extra controls

This chapter describes some additional features that are implemented within the Navier–Stokes solver `dns` to control execution and output.

4.1 Default values of flags and internal variables

There are two simple ways to establish the default values of all the internal flags and variables used by *Semtex*. The first is via the `calc` utility: run `calc -h` and check the output (this will also show you all the functions available to the parser for calculating `TOKEN` variables, initial and boundary conditions). The second is to examine the file `femlib/defaults.h`.

4.2 Checkpointing

By default, intermediate solutions are written out as checkpoint dumps in file `session.chk` every `IO_FLD` steps (default value `IO_FLD = 500`), rotating this to `session.chk.bak` so there are usually two checkpoint files available for restarting if execution stops prematurely (e.g. if terminated by a queuing system or by a floating point error). Once the final time (`N_STEP`) is reached, the outcome (the termimal solution field) is written to `session.fld`.

Sometimes however, one wants a sequence of field dumps to be written to `session.fld`. One can toggle this behaviour on the command line using `dns -chk`, or alternatively set the `TOKEN` `CHKPOINT=0` (the default being `CHKPOINT=1`). Note that turning off checkpointing can result in the generation of extremely large `session.fld` files.

4.3 Iterative solution

Two matrix solution methods are implemented for Helmholtz problems associated with the viscous substep of the time splitting. By default, direct Schur-complement solutions are used. The associated global matrices can consume quite large amounts of memory, typically much more than is required for storage of the associated field variable. Iterative (PCG) solution can also be selected, and this has the advantage that since it is matrix-free, no global matrices are required, however, solution may be slower than for the direct solver (depending on the condition number of the global matrix problem).

The token that controls the selection of matrix solution method is `ITERATIVE`. For `dns`, PCG solution can be selected for the viscous substep of the solution (`ITERATIVE = 1`). This can also be selected via a command-line option (`dns -i`), but note that this overridden by tokens set in the `session` file (the default value is `ITERATIVE = 0`).

Iterative solution can be useful for the viscous substep, particularly when the Reynolds number is high, since this decreases the condition number of the associated global matrices. In fact, iterative solutions for the viscous substep can execute faster than direct solutions at high Reynolds number,

although this is platform dependent. You should always consider trying `ITERATIVE = 1` as an option for simulations where the Reynolds number is more than a few hundred.

4.4 Wall fluxes

A file called `session.flx` is used to store the integral over the `wall` group boundaries of viscous and pressure stresses (i.e. lift and drag forces). Output is done every `IO_HIS` steps. For each direction (x, y, z), the outputs are in turn the pressure, viscous, and total force per unit length. In 2D the z-components are always zero, while in 3D the z-component pressure force is always zero, owing to the fact that the geometry is invariant in that direction. For cylindrical geometries, the output values are forces per radian (in the x and y directions) and torque per radian (in the z direction) rather than forces per unit length.

4.5 Wall tractions

If the token `IO_WSS` is set to a non-zero value then the normal and the single (2D) or two (3D) components of tangential boundary traction are computed on the `wall` group, and output every `IO_WSS` steps in the file `session.wss`. This is a binary file with structure similar to a field dump. The utility `wallmesh` is used to extract the corresponding mesh points along the walls (and can be used with `sem2tec` to produce *Tecplot* input files). Note also that there is a stand-alone utility called `traction` which is a post-processor that takes a standard `.fld` file and produces a wall traction file.

4.6 Modal energies

For three-dimensional simulations (`N_Z > 2`), a file of modal energies, `session.mdl`, is produced. This provides valuable diagnostic information for turbulent flow simulations. For each active Fourier mode k in the simulation, the value output every `IO_HIS` steps is

$$E_k = \frac{1}{2A} \int_\Omega \hat{\boldsymbol{u}}_k^* \cdot \hat{\boldsymbol{u}}_k \, \mathrm{d}\Omega,$$

where A is the area of the 2D domain Ω. (In cylindrical coordinate problems, the integrand is multiplied by radius.) Each line of the file contains the time t, mode number k and E_k.

We note that the energies are output only for non-negative Fourier modes. To get the correct estimates for the one-sided spectrum (and to satisfy Parseval's relation), the energies for non-zero modes should be doubled.

4.7 History points

History points are used to record solution variables at fixed spatial locations as the simulation proceeds. The locations need not correspond to grid points, as data are interpolated onto the given spatial locations using the elemental basis functions. Locations of history points are declared in the `session` file as follows:

```
<HISTORY NUMBER=1>
#       tag     x       y       z
        1       0       0       0
</HISTORY>
```

A file called `session.his` is produced as output. Each line of the file contains the step number, the time, the history point tag number, followed by values for each of the solution variables. The step interval at which history point information is dumped to file is controlled by the `IO_HIS` token; the default value is `IO_HIS = 10`.

4.8 Averaging

Set AVERAGE = 1 in the tokens section to get averages of field variables left in files session.ave and session.avg (which are analogous to session.chk and session.fld, but session.ave.bak is not produced). Averages are updated every IO_HIS steps, and dumped every IO_FLD steps. Restarts are made by reading session.avg if it exists.

Setting AVERAGE = 2 will accumulate averages for Reynolds stresses as well, with reserved names ABCDEF, corresponding to products

```
uu uv uw     A  B  D
   vv vw  =     C  E
      ww           F
```

The hierarchy is named this way to allow accumulation of products in 2D as well as 3D (for 2D you get only ABC). In order to actually compute the Reynolds stresses from the accumulated products you need to run the rstress utility, which subtracts the products of the means from the means of the products:

```
rstress session.avg > reynolds-stress.fld
```

An alternative function of rstress is to subtract one field file from another:

```
rstress good.fld test.fld | convert | diff
```

Setting AVERAGE = 3 will accumulate sums of additional products for computation of terms in the energy transport equation. You will then need to use the eneq utility to actually compute the terms. Presently this part of the code is only written for Cartesian coordinates.

4.9 Phase averaging

Phase averaging is useful for turbulent flows with a dominant (and known) underlying temporal period. We can collect statistics (with AVERAGE=1, 2 or 3) — much as for the case without phase averaging enabled — conditional on phase in the cycle of the underlying period, see Reynolds and Hussain (1972). Turning on phase averaging does not preclude or stop collection of standard statistics. The enabling token is N_PHASE, which must be a positive integer; in addition one needs token STEPS_P (steps per period) which must be chosen such that STEPS_P modulo N_PHASE is zero, and also N_STEP modulo N_PHASE must be zero *and* IO_FLD=STEPS_P/N_PHASE. Statistics are written to files session.0.phs ... session.X.phs where X=N_PHASE-1. The Reynolds stresses computed from these files will represent fluctuations around the conditional average flow at each phase point (the so-called 'triple decomposition').

The slight difficulty is that if the period is not very well-defined or we have a poor estimate of it, our sampling phase will slowly drift unless we take corrective action. However if the underlying period is very well defined (e.g. the flow is periodically forced) the method has great potential.

4.10 Particle tracking

The code allows for tracking of massless particles, but this only works correctly for non-concurrent execution at present. Tracking is quite an expensive operation, since Newton–Raphson iteration is used to relocate particles within each element at every timestep.

The application looks for a file called session.par. Each line of this file is of form

```
#     tag  time  ctime  x     y      z
      1    0.0   0.0    1.0   10.0   0.5.
```

The `time` value is the integration time, while `ctime` records the time at which integration was initialised.

Output is of the same form, and is called `session.trk`. The use of separate files, rather than by declaration in the session file, is intended so that `session.trk` files can be moved to `session.par` files for restarting. Particles that aren't in the domain at startup, or leave the domain during execution, are deleted.

Setting `SPAWN = 1`, re-initiates extra particles at the original positions every timestep. With spawning, particle tracking can quickly grow to become the most time-consuming part of execution.

4.11 Spectral vanishing viscosity

Spectral vanishing viscosity (SVV) amounts to implementing larger viscosity at higher wavenumbers either in Fourier space or in spectral element polynomial space. The idea is that as resolution is increased via p-refinement, the effect 'vanishes' (Tadmor; 1989; Maday et al.; 1993). One may regard SVV either as a type of implicit large-eddy simulation methodology (Pasquetti; 2006) or as a means of stabilizing spectral element solutions especially at high Reynolds numbers (Xu and Pasquetti; 2004; Kirby and Sherwin; 2006). Neither of these ideas has firm theoretical underpinning at this stage, yet the method does appear quite effective in reducing resolution requirements for turbulent flow simulations (Koal et al.; 2012; Chin et al.; 2015). Our implementation and nomenclature follows the 'standard method' described in Koal et al. (2012). One can turn on SVV separately and with different parameters for (x, y) spectral elements and in the Fourier (z) direction. These are all declared in the `TOKENS` section.

`SVV_MN`	Corresponds to cut-in mode M_{zr} in spectral elements. Must be less than `N_P`.
`SVV_MZ`	Corresponds to cut-in mode M_{φ} in Fourier direction. Must be less than `N_Z/2`.
`SVV_EPSN`	Corresponds to ε_{zr}. Should be a value larger than `KINVIS`, e.g. `5*KINVIS`.
`SVV_EPSZ`	Corresponds to ε_{φ}. A value larger than `KINVIS`.

The default polynomial transform in to place spectral element expansions into a discrete hierarchical space is the discrete Legendre transform (see e.g. Blackburn and Schmidt; 2003). This can be changed in `src/svv.cpp`.

4.12 General body forcing

This extension was developed by Thomas Albrecht.

If found, the `FORCE` section of the session file allows you to declare various types of body forcing, i.e. add a source term to the RHS of the Navier–Stokes equation. The currently implemented types include (any combination allowed):

$\boldsymbol{f} =$	$\boldsymbol{f}_{const}$	constant force
$+$	$\boldsymbol{a_1}(\boldsymbol{x})$	steady, but spatially varying force
$+$	$\boldsymbol{a_2}(\boldsymbol{x})\,\boldsymbol{\alpha}(t)$	modulated force
$-$	$m_1(\boldsymbol{x})\,(\boldsymbol{u}-\boldsymbol{u}_0)$	sponge region
$-$	$m_2(\boldsymbol{x})\,(\boldsymbol{u}/\lvert\boldsymbol{u}\rvert)\,\lvert\boldsymbol{u}(\boldsymbol{x},t)\rvert^2$	'drag' force
$+$	$\boldsymbol{\epsilon} G$	white noise
$-$	$\chi(\boldsymbol{u}-\overline{\boldsymbol{u}})$	selective frequency damping
$-$	$2\,\boldsymbol{\Omega}\times\boldsymbol{u}-(\mathrm{d}\boldsymbol{\Omega}/\mathrm{d}t)\times\boldsymbol{x}-\boldsymbol{\Omega}\times\boldsymbol{\Omega}\times\boldsymbol{x}$	Coriolis force.

For example, a force constant in time and space $\boldsymbol{f} = \boldsymbol{f}_{const}$ is declared by:

```
<FORCE>
        CONST_X = 4
        CONST_Y = 0
        CONST_Z = 0
</FORCE>
```

This type of forcing must not be time or space dependent. It is suitable for periodic channel flow, where you have a uniform and steady force driving the flow, see `channel-FX` for an example session.

Except for the constant force, all forcing terms are applied in physical space.

Unless otherwise noted, any skipped keyword defaults to 0. Any line starting with a hash # is ignored.

4.12.1 Steady force

A spatially varying, steady force $\boldsymbol{f} = \boldsymbol{a}(\boldsymbol{x})$, computed (or read from a file) during pre-processing and applied every time step. See `box-steady` for the complete example session. It suits applications requiring localised, steady forcing.

```
<FORCE>
        STEADY_X =  cos(x)
        STEADY_Y = -sin(z)
        STEADY_Z = -cos(y)
        # STEADY_FILE = box-steady.force.fld
</FORCE>
```

You may also point `STEADY_FILE` to a field file, in which case the force is taken from the `uvw` fields of that file and `STEADY_[XZY]` is ignored.

4.12.2 Modulated force

A spatially varying force, which is modulated in time, $\boldsymbol{f} = \boldsymbol{a}(\boldsymbol{x})\,\boldsymbol{\alpha}(\boldsymbol{t})$. The steady part $\boldsymbol{a}(\boldsymbol{x})$ is computed (or read from a file) during pre-processing, while $\boldsymbol{\alpha}(\boldsymbol{t})$ is evaluated each time step.

```
<FORCE>
        # -- spatially varying part
        MOD_A_X =  cos(x)
        MOD_A_Y = -sin(z)
        MOD_A_Z = -cos(y)
        # MOD_A_FILE = box-mod.force.fld

        # -- time varying part
        MOD_ALPHA_X = step(t, 10)
        MOD_ALPHA_Y = step(t, 10)
        MOD_ALPHA_Z = step(t, 10)
</FORCE>
```

4.12.3 Sponge region

This implements a so-called 'sponge region' defined by the shape function $m(x)$ in which a (physically meaningless) penalty term $\boldsymbol{f} = m(\boldsymbol{x})\,(\boldsymbol{u} - \boldsymbol{u}_0)$ forces the flow towards a given solution $\boldsymbol{u}_0$. It is especially useful for inflow–outflow simulations of vortex shedding or turbulence: if the velocity fluctuations hit the outflow boundary condition, they cause unphysical reflections back into the domain which distort the upstream flow. A sponge region placed just upstream the outflow boundary helps to reduce the velocity fluctuations to (near) zero and thereby prevents those reflections. The

following section would apply the penalty term for $20 \leq x \leq 24$, and within that region forces the velocity to approach $(1, 0, 0)$. That given solution may be a function of space, but must be steady.

```
<FORCE>
        SPONGE_M = 5. * step(x,20)*heav(24-x)
        SPONGE_U = 1
        SPONGE_V = 0
        SPONGE_W = 0
</FORCE>
```

4.12.4 'Drag' force

An approximate drag force $\boldsymbol{f} = -m(\boldsymbol{x})\,(\boldsymbol{u}/|\boldsymbol{u}|)\,|\boldsymbol{u}(\boldsymbol{x}, t)|^2$. Be aware that we use the previous time step's velocity $\boldsymbol{u}^n$ here.

```
<FORCE>
        DRAG_M = heav((x-2)^2 + y^2, 0.25)
</FORCE>
```

4.12.5 White noise force

Similar to the `noiz` tool, this continuously adds random perturbation $\boldsymbol{f} = (\epsilon_x, \epsilon_y, \epsilon_z)^T\, G$ in specified direction, where G is a normal distributed random variable. Setting `WHITE_MODE` ≥ 0 perturbs the given mode only, i.e. `WHITE_MODE = 2` will perturb mode 2 only. Omitting this keyword or setting `WHITE_MODE` < 0 will apply white noise to all modes.

The following example applies white noise in $x-$direction to mode 0:

```
<FORCE>
        WHITE_MODE = 0
        WHITE_EPS_X = 0.1
        WHITE_EPS_Y = 0
        WHITE_EPS_Z = 0
</FORCE>
```

Adding white noise in all three directions degrades performance by about 10%.

4.12.6 Selective frequency damping (SFD)

This is a means of obtaining an approximate steady state solution to the Navier–Stokes equations using an unsteady solver, originally described by Åkervik et al. (2006). SFD applies a penalty term of the form $-\chi(\boldsymbol{u} - \overline{\boldsymbol{u}})$ to the right-hand side of the momentum equations, where $\overline{\boldsymbol{u}}$ is an estimate of the time-mean solution that is updated as integration proceeds (and held in internal storage). SFD can also be considered as applying an IIR low-pass digital filter to the discrete approximation of the Navier–Stokes equations.

The two parameters are `SFD_CHI` (i.e. penalization multiplier χ) and `SFD_DELTA`, which is the time constant Δ used in updating a forwards-Euler approximation of the steady flow $\overline{\boldsymbol{u}}$ (see reference). Both values are problem-specific and should be tuned to get acceptable results. Note that it is not always possible to obtain a steady outcome with SFD, and that it is generally preferable to use standard skew-symmetric form of the nonlinear terms for `dns`, rather than the now-default alternating skew symmetric form: this can be achieved by setting token `ADVECTION = 0` or by using command-line flag `-S` with `dns`.

```
<FORCE>
        SFD_CHI   = 0.2
```

```
        SFD_DELTA = 0.75
</FORCE>
```

4.12.7 Rotating frame of reference: Coriolis and centrifugal force

If the flow is to be computed in a rotating frame of reference, additional acceleration terms appear, namely $\boldsymbol{f} = -2\,\boldsymbol{\Omega} \times \boldsymbol{u} - (\mathrm{d}\boldsymbol{\Omega}/\mathrm{d}t) \times \boldsymbol{x} - \boldsymbol{\Omega} \times (\boldsymbol{\Omega} \times \boldsymbol{x})$ (Batchelor; 1967). The vector of rotation $\boldsymbol{\Omega}$ is *always* given in Cartesian co-ordinates, even if `CYLINDRICAL = 1`. Its magnitude and/or orientation can change with time. However, the axis of rotation it is always assumed to go through the origin. Depending on whether $\boldsymbol{\Omega}$ is steady or not, usage slightly differs.

For unsteady $\boldsymbol{\Omega}$, set the flag `CORIOLIS_UNSTEADY = 1` and give $\boldsymbol{\Omega}$ and $\mathrm{d}\boldsymbol{\Omega}/\mathrm{d}t$. All terms are re-evaluated each time step.

```
<TOKENS>
        f        = 1.
        omega    = TWOPI * f
</TOKENS>

<FORCE>
        CORIOLIS_UNSTEADY = 1

        CORIOLIS_OMEGA_X = 0
        CORIOLIS_OMEGA_Y = 0
        CORIOLIS_OMEGA_Z = omega * sin(t)

        CORIOLIS_DOMEGA_X_DT = 0
        CORIOLIS_DOMEGA_Y_DT = 0
        CORIOLIS_DOMEGA_Z_DT = omega * cos(t)
</FORCE>
```

For constant $\boldsymbol{\Omega} \neq f(t)$, the term $-(\mathrm{d}\boldsymbol{\Omega}/\mathrm{d}t) \times \boldsymbol{x}$ vanishes, and the centrifugal force $-\boldsymbol{\Omega} \times (\boldsymbol{\Omega} \times \boldsymbol{x})$ can be computed during pre-processing. Set `CORIOLIS_UNSTEADY = 0` and make sure to include the centrifugal force manually using a steady force as it is no longer computed automatically[1]. A temporal derivative $\mathrm{d}\boldsymbol{\Omega}/\mathrm{d}t$, if given, is ignored.

```
<FORCE>
        CORIOLIS_UNSTEADY = 0

        CORIOLIS_OMEGA_X = 0
        CORIOLIS_OMEGA_Y = 0
        CORIOLIS_OMEGA_Z = omega

        # -- centrifugal term for Omega = (0, 0, omega)^T
        #    for a cylindrical problem
        STEADY_X = x*omega^2
        STEADY_Y = omega^2*y*(cos(z)^2)
        STEADY_Z = -omega^2*y*cos(z)*sin(z)
</FORCE>
```

See Albrecht et al. (2015) for an example of DNS carried out in a rotating frame of reference.

[1] If you're lazy, or for cross-checking, you could set `CORIOLIS_UNSTEADY = 1` and omit `CORIOLIS_DOMEGA_[XYZ]_DT` to have the centrifugal term computed automatically. Note, however, that this degrades performance as it is done each time step.

Chapter 5

Specialised executables

The special compilations below can be combined.

5.1 Concurrent execution

The code supports concurrent execution for 3D simulations, with MPI used as the message-passing kernel. Compile using `make MPI=1` to produce `dns_mp`. (You will also need to compile in the appropriate message-passing routines in compiling `femlib`, for which change to the `femlib` directory, then do `make clean; make MPI=1; make install MPI=1`.) Nonlinear terms are not dealiased when running in parallel, but are dealiased in the Fourier direction when running on one process, or running the serial code. To get a serial code that does not perform dealiasing on Fourier terms (e.g. for cross-checking), compile the serial code using `make ALIAS=1` to produce `dns_alias` (in which case make sure you delete `nonlinear.o` first).

5.2 Vector architectures

The code has a fair amount of low-level optimisation built in for vector computer architectures, but it's not compiled in by default. To get vector-optimised routines, add `-D_VECTOR_ARCH` to the section of `src/Makefile` appropriate to your machine. Also you may want to try altering the parameter `LVR` in `src/temfftd.F` if your job makes heavy use of FFTs.

Chapter 6

Code design and the Semtex API

This chapter is in development.

While the top level of the code is written in C++, the bulk of computational work is carried out using 3rd-party libraries: BLAS and LAPACK (vendor- or distribution-supplied) for 2D operations, Temperton's 2-3-5 prime factor FFT (incorporated into `femlib`) for 3D operations, and (open)MPI for parallel operations. Depending on what your application hits the hardest, one or other of these things may be the speed-determining component. Optimizing compilers are liable to make a only a small difference — most speed-up is now to be achieved by algorithm development.

Some fundamental design decisions:

1. Most real-type data arrays are flat, 1D, zero-indexed, i.e. the same as employed in FORTRAN, and this makes them easy to use with FORTRAN routines.

2. The layout of these flat arrays are typically taken as row-major, which is standard C/C++. However, FORTRAN uses column-major ordering. For this reason, any BLAS or LAPACK operation may at first sight seem to be the transpose of what is intended.

3. Most low-level C++ methods in the code do not incorporate internal data storage but can be regarded as operator routines, and get handed addresses to appropriate parts of storage from within the flat data arrays on which to work.

Coding conventions:

1. Class private or protected member data names start with an underscore, e.g. `_ntot`.

6.1 Useful things to know about

1. Directory layout. The following directories are present in the distribution: `include` which has copies of header files; `src` which holds C++ source code for the classes shared by *Semtex* applications; `veclib` which holds routines for many standard loops over vectors, with a mnemonic naming convention (the code here is almost exclusively written in C); `femlib` has one-dimensional spectral polynomial routines (knot and quadrature point computations, differentiation matrix construction) and FFTs, all written in either C or FORTRAN77; `utility` routines for pre and post-processing; `test` which has code validity regression tests, with the 'right answers' stored in `regress`; `mesh` holds a selection of session files. The two main application code directories are `elliptic` and `dns` which have been described in earlier chapters. The `sm` directory contains useful *SuperMongo* macros.

2. Hierarchy of main data storage: domain, fields, auxfields, elements. The key entity for most applications programming is the `AuxField` class, which contains scalar field variables and a

list of `Element` pointers. The `Field` class inherits from the `AuxField` class, adding a list of boundary condition applicators and the ability to solve elliptic problems. The `Domain` class holds an array of `Field` pointers and most of its internal storage is publicly accessible.

3. Nodal elements: the shape functions used in the code correspond to the classical 'nodal', rather than the 'modal' scheme. This means that the shape functions are tensor products of 1D Lagrange interpolants that have value unity at one mesh node and zero at the others.

4. *Timestepping algorithm and the code loop* The scheme is the 'stiffly stable' scheme, based on backward differencing in time, and uses time-splitting, see Karniadakis et al. (1991). What is stored where, and when — see figure 6.1.

5. *Boundary conditions, use of inheritance* Distinction between the way BCs are dealt with. Periodicity not a boundary condition.

6. Support libraries and static member functions. BLAS-conformant increments.

7. The parser and what things can be parsed.

8. What is done in the driver routine and the basic idea of code layout.

9. *Implications of Fourier transform in one direction* For 3D computations, note that for all of the timestepping loop, other than during computation of the nonlinear terms, field variables are help in the Fourier-transformed state.

10. Tensor-product derivative operations.

11. Direct versus iterative solves.

12. Static condensation.

13. Message passing and data exchange.

6.2 Altering the code

If you want to alter the supplied source code, the first thing you need to know is that `make` will seek to resolve source file names in the current directory first, before looking elsewhere (e.g. the `src` directory, the `include` directory). This means that the best strategy is to copy (if not already present) *only* the relevant files which you need to change into your current development directory, typically from the `src` directory, and alter these. This way your new version does not interfere with the supplied code base, and it is also readily apparent exactly which files you have had to change.

For example, say you want to add some new functionality to the `AuxField` class, within the `dns` application. Make a clean copy of the source files (`Makefile`, `*.C`, `*.h`) in `dns` to another directory at the same level. In that directory, place copies of `auxfield.C` and (if required) `auxfield.h` from `../src` and then work on these.

Testing. Typically when adding code features you want to be sure that you haven't broken existing functionality. The easy way to check is to use the `testregress` script in the `test` directory. It will tell you if the code passes or fails standard regression tests which exercise most code features.

	Domain				Us			Uf		
STAGE	D->u[0] u	D->u[1] v	D->u[2] w	D->u[3] p	Us[.][0]	Us[.][1]	Us[.][2]	Uf[.][0]	Uf[.][1]	Uf[.][2]
Start	u^n	v^n	w^n	p^n	— / u^{n-1}	— / v^{n-1}	— / w^{n-1}	— / U_{fx}^{n-1}	— / U_{fy}^{n-1}	— / U_{fz}^{n-1}
end nonLinear	—	—	—	—	u^n / u^{n-1}	v^n / v^{n-1}	w^n / w^{n-1}	U_{fx}^n / U_{fx}^{n-1}	U_{fy}^n / U_{fy}^{n-1}	U_{fz}^n / U_{fz}^{n-1}
end waveProp	u^*	v^*	w^*	—	u^n / u^{n-1}	v^n / v^{n-1}	w^n / w^{n-1}	U_{fx}^n / U_{fx}^{n-1}	U_{fy}^n / U_{fy}^{n-1}	U_{fz}^n / U_{fz}^{n-1}
start setPForce	u^n	v^n	w^n	—	u^* / u^{n-1}	v^* / v^{n-1}	w^* / w^{n-1}	— / U_{fx}^n	— / U_{fy}^n	— / U_{fz}^n
end setPForce	u^n	v^n	w^n	—	u^* / u^{n-1}	v^* / v^{n-1}	w^* / w^{n-1}	$\nabla\cdot\boldsymbol{u}/\Delta t$ / U_{fx}^n	— / U_{fy}^n	— / U_{fz}^n
end Solve (P)	u^n	v^n	w^n	p^{n+1}	u^* / u^{n-1}	v^* / v^{n-1}	w^* / w^{n-1}	— / U_{fx}^n	— / U_{fy}^n	— / U_{fz}^n
end project	u^n	v^n	w^n	p^{n+1}	— / u^{n-1}	— / v^{n-1}	— / w^{n-1}	$\frac{-u^{**}}{\nu\Delta t}$ / U_{fx}^n	$\frac{-v^{**}}{\nu\Delta t}$ / U_{fy}^n	$\frac{-w^{**}}{\nu\Delta t}$ / U_{fz}^n
update velocity storage	u^n	v^n	w^n	p^{n+1}	— / u^n	— / v^n	— / w^n	$\frac{-u^{**}}{\nu\Delta t}$ / U_{fx}^n	$\frac{-v^{**}}{\nu\Delta t}$ / U_{fy}^n	$\frac{-w^{**}}{\nu\Delta t}$ / U_{fz}^n
end solve (U)	u^{n+1}	v^{n+1}	w^{n+1}	p^{n+1}	— / u^n	— / v^n	— / w^n	— / U_{fx}^n	— / U_{fy}^n	— / U_{fz}^n

Figure 6.1: Arrangement of internal storage during timestepping loop (see `dns/integrate.C`) for a three-velocity-component, second-order-time, stepping scheme. Presence of a '-' indicates that the relevant storage is free for over-writing if desired. Diagonal lines divide the upper- and lower-order storage so that e.g. the first entry under column labelled `Us[.][0]` corresponds (above diagonal) to `Us[0][0]` and (below) to `Us[1][0]`. The number of levels corresponds to `N_TIME`; i.e. what is shown here corresponds to `N_TIME=2`. For `N_TIME=1` the entries below the diagonals do not exist, while for `N_TIME=3`, there would be an additional level for $n-2$-type entries. If the problem is three-dimensional (`N_Z>1`), field variables are held in the Fourier-transformed state except during computation of nonlinear terms (where products are computed in physical space).

Chapter 7

DNS 101 — Turbulent channel flow

This chapter was largely the contribution of Peter Kulb from TU-Dresden. It is intended as a introductory guide for those contemplating DNS of a turbulent flow.

Turbulent Poiseuille flow between two parallel plates is a canonical test case for direct numerical simulation (DNS) codes. While *Semtex* will of course deal with more complicated problems, we'll use this as an example to illustrate techniques of mesh design, and of obtaining transition and extracting turbulence statistics. Our basis for comparison will be the DNS results of Kim, Moin and Moser (1987), obtained with a Fourier–Fourier–Chebyshev code.

A schematic of the configuration is shown with figure 7.1. The flow is assumed periodic in the x (streamwise) and z (spanwise) directions. In the y-direction, non-slip Dirichlet boundary conditions are applied for all velocity components at the upper and lower walls, where also a high-order pressure boundary condition (of computed Neumann type, see Karniadakis et al.; 1991) is employed. Since we are working with a spectral element–Fourier code, we are free to choose either of the x or z directions as the Fourier direction; here, we will use Fourier expansions in the z direction, have a spectral element mesh in the x–y plane, and set up explicit periodicity in the x direction.

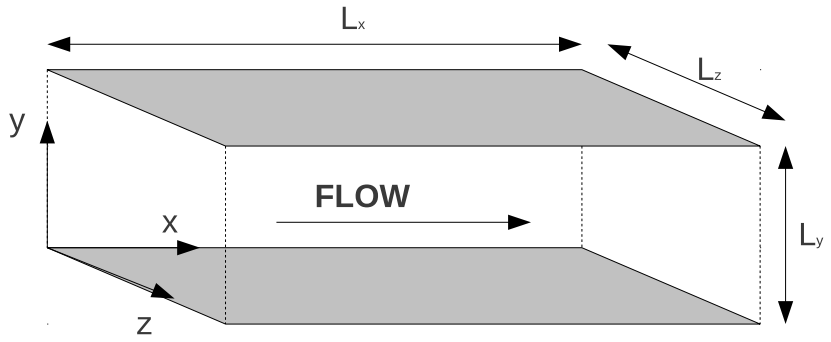

Figure 7.1: Channel flow geometry.

7.1 Parameters

To match Kim et al. (1987) we will aim for a bulk flow Reynolds number based on the centreline mean speed U and channel half-height $\delta = L_y/2$ of $Re_\delta = U\delta/\nu = 3300$. For this flow the associated Reynolds number based on the friction velocity $u_\tau = (\tau_w/\rho)^{1/2}$ and half-height is $Re_\tau = u_\tau\delta/\nu = 183$. (It is worth noting that the relationship between the bulk and friction Reynolds numbers for turbulent flows is empirically based. For channel flow, a reasonable approximation is given by $Re_\delta/Re_\tau = 2.5\ln Re_\tau + 5$, while for turbulent flow in a pipe of diameter D, Blasius' correlation

$Re_\tau = u_\tau D/2\nu = 99.44 \times 10^{-3} Re_D^{7/8}$ is quite good at moderate Reynolds numbers.)

Kim et al. (1987) used domain extents of $L_x = 4\pi\delta$ and $L_z = 2\pi\delta$ but for illustrative purposes we will choose the smaller sizes $L_x = 2\pi\delta$ and $L_z = \pi\delta$. We will find that the turbulence statistics examined are apparently little affected by this reduction in domain size, but the cost of simulation is significantly reduced. Since we will use Fourier expansions in the z direction we will have the basic spanwise wavenumber $\beta = 2\pi/L_z = 2$. This is set below by the simulation token `BETA = 2`.

We will choose second-order time integration, usually the best compromise between stability and accuracy. (This is set below by the token `N_TIME = 2`, which could actually be omitted from the session file since that is the default value.)

We need to choose a spectral element polynomial order. Values around 9 provide a good compromise between speed and accuracy for this code. This is set with the token `N_P = 10` (the number of points along the edge of an element, one more than the polynomial order). Sometimes in what follows we will also approximate the typical number of mesh divisions along the the edge of an element as 10, although the sharp-eyed reader will note that it should logically be 9.

We need to choose the kinematic viscosity, ν. We aim to have $Re_\delta = 3300$. It is good simulation/numerical practice to aim for a characteristic velocity scale of unity, as well as a characteristic mesh length scale of unity. In this case these goals imply that we aim for a centreline mean speed $U \simeq 1$ and our channel half-height $\delta = 1$. With these choices we are left with

$$\nu = Re_\delta^{-1} = 303 \times 10^{-6},$$

which is set by the simulation token `KINVIS = 303e-6`.

When using periodicity in the streamwise direction, a body force is required in order to maintain the flow. This is needed because the pressure as well as the velocity is required to be streamwise-periodic. The required body force per unit mass (i.e. acceleration) is calculated from a time-average force balance in x-direction for the entire channel

$$\begin{aligned} \rho \times f_x \times \underbrace{\cancel{L_x} \times L_y \times \cancel{L_z}}_{\text{channel volume}} &= 2 \times \tau_w \times \underbrace{\cancel{L_x} \times \cancel{L_z}}_{\text{one wall surface}} \\ \rho \times f_x \times \delta &= \tau_w \\ \frac{f_x \delta}{U^2} &= \left(\frac{u_\tau}{U}\right)^2 = \left(\frac{Re_\tau}{Re_\delta}\right)^2 \end{aligned}$$

where τ_w is the time-average wall shear stress. With $\rho = \delta = U = 1$ and (from correlation/previous results) $Re_\tau = 183$, $Re_\delta = 3300$, the required value is

$$f_x = 3.08 \times 10^{-3}.$$

This will be set with the token `CONST_X = 3.08e-3` in the `<FORCE>` section. Note that if required for body forces in the y or z directions there are corresponding tokens `CONST_Y` and `CONST_Z` respectively (see section 4.12 for other types of forcing). These body forces are added to the component momentum equations (the Navier–Stokes equations). Also note that the code is written assuming $\rho = 1$.

The friction velocity $u_\tau = (\tau_w/\rho)^{1/2} \equiv U Re_\tau / Re_\delta = 55.5 \times 10^{-3}$, and the viscous wall length scale $l_w = \nu/u_\tau = 5.46 \times 10^{-3}$.

7.2 Mesh design

In designing the mesh for the channel flow, rules of thumb established in related studies (Piomelli; 1997; Kim et al.; 1987; Blackburn and Schmidt; 2003) have been considered. All mentioned coordinates are with respect to coordinate system established in this work. Thus, x is the streamwise

direction, y the wall-normal and z the spanwise direction — Fourier expansions are always used in the z direction.

Kim et al. (1987) used $\Delta x^+ = \Delta x/l_w = 12$, $y^+ = 0.05$ (at the wall) and $\Delta z^+ = 7$ in their study. (Piomelli; 1997) proposed similar values with $\Delta x^+ = 15$, $\Delta y^+ < 1|_{\text{wall}}$ and $\Delta z^+ = 6$.

The wall-normal part of the spectral element mesh design strategy for wall-resolved LES described by Blackburn and Schmidt (2003) is to terminate the element closest to the wall at $y^+ = 10$, the second element at $y^+ \simeq 35$, then use a geometric progression of sizes to reach the flow centreline (one has to choose the number of elements and geometric expansion factor). This ensures there is good resolution in the viscous-dominated wall layer as well as the buffer layer ($10 < y^+ < 35$), where turbulent energy production is greatest. Nevertheless, here, the second element layer is reduced to $y^+ = 25$ in order to improve resolution in the middle of the buffer layer.

The first two element heights in the wall-normal direction are then $\Delta y_1(10) = 0.056$ and $\Delta y_2(25) = 0.139$. For the remainder, we use a geometric progression of four elements starting with an initial height of $\Delta y = 0.139 - 0.056 = 0.083$ to reach the channel centreline. The total number of elements in the y-direction is 12.

Next considering the x-direction, the indicative mesh spacing is $\Delta x^+ = 15$, corresponding to a length $\Delta x = 15 \times 5.46 \times 10^{-3} = 81.9 \times 10^{-3}$. The number of grid points needed to cover the domain extent in the x-direction is then of order $N_x = 2\pi/\Delta x = 76.7$. For a mesh with `N_P=10` we need of order 8 elements. So our (x, y) spectral element mesh is now of size $8 \times 12 = 96$ elements.

Finally considering the z direction, we have $L_z = \pi$ and want $\Delta z^+ \simeq 7$, or $\Delta z \simeq 7 \times 5.46 \times 10^{-3} = 38.2 \times 10^{-3}$. The implied number of z planes is then of order $\pi/38.2 \times 10^{-3} = 82.2$. We need an integer number of planes which must be even (one prime factor of 2) and other allowable prime factors of 3 and 5. 80 planes seems convenient so we choose `N_Z = 10`. Note that means we could run on either a single processor in serial execution or 2, 4, 8, 10, 20 or 40 in parallel. There will be 40 Fourier modes.

The mesh can be created using the provided tool `rectmesh` which reads from an input file containing two blocks with all grid lines in x and y separated by an empty line. The output from running `rectmesh` will be a valid *Semtex* session file but which will generally need some editing.

```
rectmesh [options] mesh.inp > sessionfile
```

A `rectmesh` input file for this case is as follows:

```
-3.14159265358979
-2.35619449019234
-1.5707963267949
-0.785398163397448
0.0000
0.785398163397448
1.5707963267949
2.35619449019234
3.14159265358979

-1.0
-0.944
-0.861
-0.745
-0.575
-0.330
0.0
0.330
0.575
0.745
0.861
0.944
```

```
1.0
```

Once this file is built, all the above mentioned parameters can be changed to their desired value. Also, the boundary conditions have to be named and set into place. We use wall boundary conditions on the upper and lower edges of the domain, and edit the <SURFACES> section to obtain periodicity in the streamwise direction. Here the example input file for this particular case:

```
#################################################################
#  96 element channel flow, for Re_bulk = 3300, Re_tau = 183

<FIELDS>
u v w p
</FIELDS>

<USER>
u = 1.0-y*y
v = 0.0
w = 0.0
p = 0.0
</USER>

<TOKENS>
N_TIME = 2
N_P    = 10
N_Z    = 80
BETA   = 2.0
N_STEP = 60000
D_T    = 0.002
KINVIS = 303e-6
IO_CFL = 100
IO_HIS = 100
AVERAGE = 2
</TOKENS>

<FORCE>
CONST_X = 3.08e-3
</FORCE>

<GROUPS NUMBER=1>
1 w wall
</GROUPS>

<BCS NUMBER=1>
1 w 4
<D> u = 0.0 </D>
<D> v = 0.0 </D>
<D> w = 0.0 </D>
<H> p       </H>
</BCS>

<NODES NUMBER=117>
    1        -3.14159             -1              0
  ...
  117         3.14159              1              0
</NODES>

<ELEMENTS NUMBER=96>
    1 <Q>    1    2   11   10    </Q>
```

```
  ...
   96 <Q>  107  108  117  116    </Q>
</ELEMENTS>

<SURFACES NUMBER=28>
    1    1    1    <B> w </B>
    2    2    1    <B> w </B>
    3    3    1    <B> w </B>
    4    4    1    <B> w </B>
    5    5    1    <B> w </B>
    6    6    1    <B> w </B>
    7    7    1    <B> w </B>
    8    8    1    <B> w </B>
    9   89    3    <B> w </B>
   10   90    3    <B> w </B>
   11   91    3    <B> w </B>
   12   92    3    <B> w </B>
   13   93    3    <B> w </B>
   14   94    3    <B> w </B>
   15   95    3    <B> w </B>
   16   96    3    <B> w </B>
   17    8    2    <P>   1      4       </P>
   18   16    2    <P>   9      4       </P>
   19   24    2    <P>  17      4       </P>
   20   32    2    <P>  25      4       </P>
   21   40    2    <P>  33      4       </P>
   22   48    2    <P>  41      4       </P>
   23   56    2    <P>  49      4       </P>
   24   64    2    <P>  57      4       </P>
   25   72    2    <P>  65      4       </P>
   26   80    2    <P>  73      4       </P>
   27   88    2    <P>  81      4       </P>
   28   96    2    <P>  89      4       </P>
</SURFACES>

<HISTORY NUMBER=1>
1 0.0 0.0 0.0
</HISTORY>
```

7.3 Initiating and monitoring transition

The critical bulk Reynolds number for linear instability of channel flow is $Re_c = 5772$ but turbulence can typically be maintained down to lower values (and here we are aiming at $Re_\delta = 3300$) if transition is obtained. Our strategy here will be to start from a laminar flow profile and add some white noise to obtain transition. This is done using the following single line to generate an initial condition:

```
compare chan | noiz -p 0.1 chan.fld > chan.rst
```

Here, the command-line value 0.1 represents the standard deviation of the normal/Gaussian distribution from which the noise is derived using a pseudorandom number generator and is therefore quite large compared to an average velocity of $U = 1$. It is necessary, since our Reynolds number is here below the critical value, to assure a sufficient amount of disturbance to initiate transition to a turbulent state. If the Reynolds number were above the critical value, any perturbation level above machine noise level should eventually produce transition — it just depends on how long you are prepared to wait. We note that channel flow is a case for which it is relatively easy to obtain transition to turbulence without carefully manipulating the noise level, or restricting the time step.

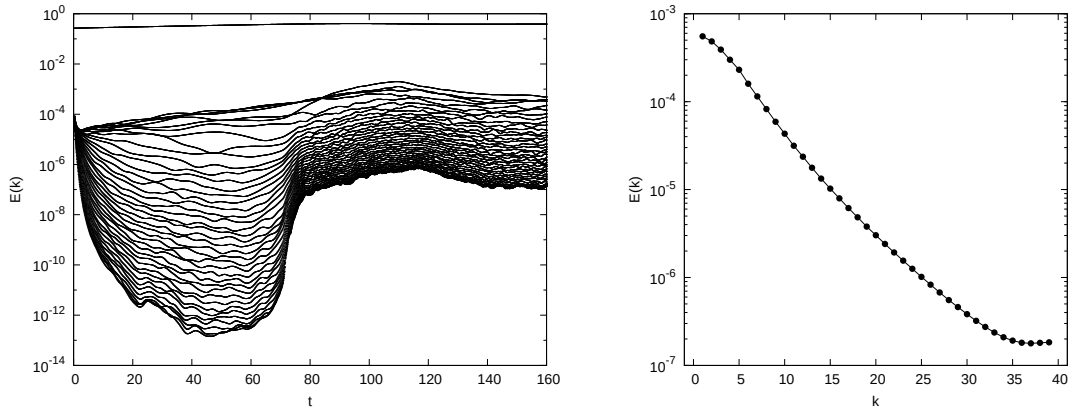

Figure 7.2: Modal energies for (a) the individual wave numbers over time and (b) by wavenumber.

In order to monitor transition, a very useful diagnostic is to monitor the evolution of kinetic energies in all Fourier modes. Transition should be easy to see as a moderately rapid increase in turbulent energy within small scales that are represented by higher wave numbers. Figure 7.2(a) shows the transition for the mentioned channel flow. Figure 7.2(b) indicates that the resolution is adequate due to a separation of about three and a half decades between the highest and smallest wave number. An increase of energy within the highest wave numbers would also indicate an under-representation because of aliasing of the energy of higher modes back into the resolved frequency domain (which is the underlying reason for the plateau seen at the highest wavenumbers in figure 7.2(b)).

Figure 7.2(a) shows the evolution of kinetic energies in the 40 Fourier modes represented. By way of interpretation, the mode with highest energy (here, and typically) is mode 0, which represents the two-dimensional or z-average flow. All the other modes start off with much the same energy, which is a result of having chosen to pollute all modes equally when using the `noiz` utility (often, one would just pollute mode 1 and allow convolution to distribute energy to all other modes — this gives a more gentle perturbation). The highest modes typically decay rather rapidly initially, with the lower modes either slowly losing or (as here, gaining) energy. Also the energy in mode 0 here increases a little over time, partly because the initial condition here actually had a lower volumetric flow rate than the equilibrium turbulent flow. At $t \approx 70$ the flow makes a transition to a turbulent state, typically signalled by the higher modes gaining energy fairly rapidly until a quasi-equilibrium is reached. Eventually the flow settles to a statistical equilibrium at $t \approx 140$. Figure 7.2(b) shows the temporal average values of energies in the various Fourier modes. (The *SuperMongo* macros `moden` and `modav` were used to plot figure 7.2.)

7.4 Flow statistics

Flow statistics can be collected by setting the `AVERAGE` token to non-zero values 1, 2 or 3 (here a value of 2 was used, see below). See also § 4.8. To obtain statistical convergence it is necessary to average over a sufficiently long time, just as would be the case in a physical experiment. Statistics are updated every `IO_HIS` simulation steps (here, every 100 steps). In the present case, the total averaging time was chosen to be 400, which represents of order 60 'wash-through' times, since the domain length is 2π and the bulk flow speed $U = 1$. Since the time between data updates is $100 \times 0.002 = 0.2$ there are a total of $400/0.2 = 2000$ averaging buffer updates.

Once the simulation is run, a `.avg` file is produced. For `AVERAGE=1`, statistics for the represented fields are collected, i.e. $\langle u \rangle$, $\langle v \rangle$, $\ldots$, $\langle p \rangle$. For `AVERAGE=2`, averages of velocity field products are stored too, i.e. $\langle uu \rangle$, $\langle uv \rangle$, etc. For `AVERAGE=3`, additional products are collected to allow computation of terms in the fluctuating energy equation. Note that it is necessary to calculate

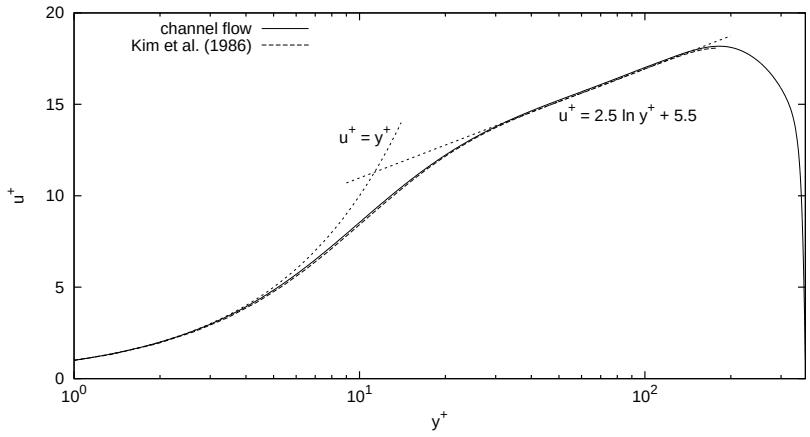

Figure 7.3: Mean velocity profile of the channel flow compared to the law of the wall and data from Kim et al. (1987)

Reynolds stresses and energy equation terms in post-processing (e.g. $\langle u'v' \rangle = \langle uv \rangle - \langle u \rangle \langle v \rangle$). Note also that if `.avg` files exist, they are read in at start of execution of `dns` to initiate averaging buffers: the `Step` value in the file's header stores the number of averages obtained to date.

Having collected statistics, our next step is to calculate the Reynolds stresses and to average in x- and z-direction. To illustrate the possible processing, here is an example shell script:

```
#!/bin/bash

# temporary files
FTNZ='/tmp/chan_nz1'
FTRS='/tmp/reynolds-stress.xy'
FRSY='./reynolds-stress.y'

# average field results in z
project -z1 chan.avg > /tmp/chan.avg.xy

# calculate reynolds-stresses (xy-plane)
rstress /tmp/chan.avg.xy > $FTRS

# new input file with NZ=1
LNZ=$(cat cube | grep N_Z -n | awk -F: '{print $1}')
sed '$LNZs/.*/  N_Z    = 1/' <chan >$FTNZ

# average reynolds-stresses in x
rayavg npts navg y_0 x_0   y_0 x_1 dy dx $FTNZ $FTRS >  $FRSY
rayavg npts navg y_0 x_1   y_0 x_2 dy dx $FTNZ $FTRS >> $FRSY
...
rayavg npts navg y_0 x_n-1 y_0 x_n dy dx $FTNZ $FTRS >> $FRSY

# PLOTTING
gnuplot ~/scripts/plot_rstress.gpl;
```

Figure 7.3 shows the mean velocity profile for the channel flow in comparison to data from Kim et al. (1987). The dashed lines are representing the linear respectively logarithmic part of the law of the wall. Figure 7.4 show rms Reynolds stress values in friction velocity units with comparison to data from Kim et al. (1987). Quite good agreement is evident.

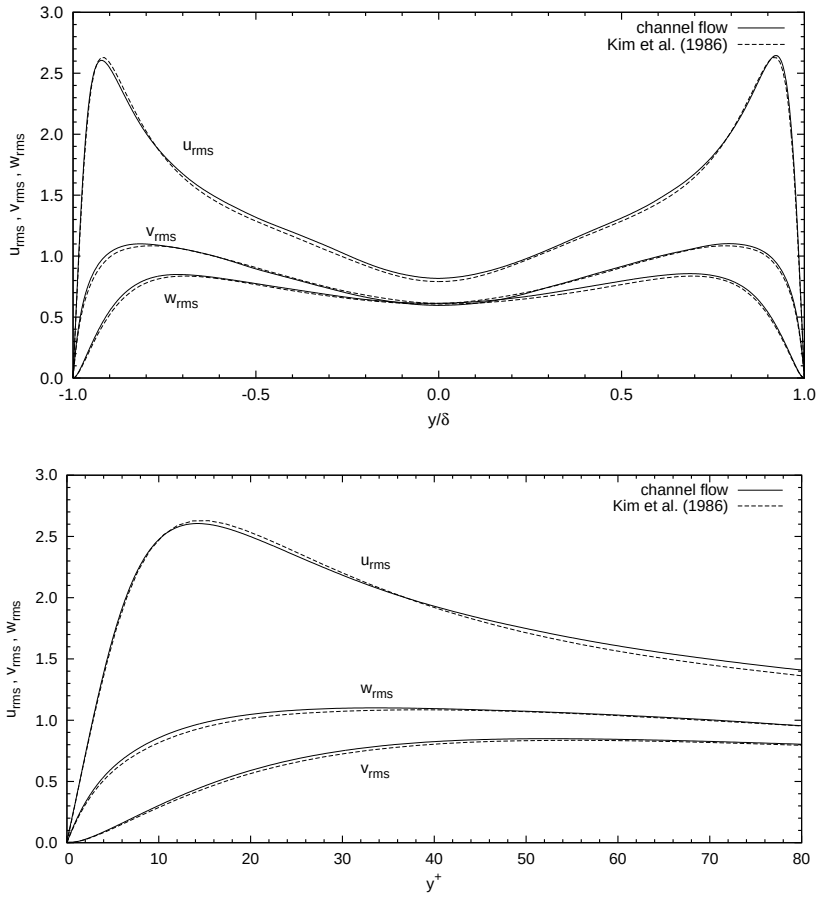

Figure 7.4: Root-mean-squares velocity fluctuations in global coordinates normalized by the wall shear velocity u_τ. Comparison to data from Kim et al. (1987).

Bibliography

Åkervik, E., Brandt, L., Henningson, D. S., Hœpfner, J., Marxen, O. and Schlatter, P. (2006). Steady solutions to the Navier–Stokes equations by selective frequency damping, *Phys. Fluids* **18**: 068102–1–4.

Albrecht, T., Blackburn, H. M., Lopez, J. M., Manasseh, R. and Meunier, P. (2015). Triadic resonances in precessing rapidly rotating cylinder flows, *J. Fluid Mech.* **778**: R–1–11.

Amon, C. H. and Patera, A. T. (1989). Numerical calculation of stable three-dimensional tertiary states in grooved-channel flow, *Phys. Fluids A* **1**(2): 2005–2009.

Batchelor, G. K. (1967). *An Introduction to Fluid Dynamics*, Cambridge University Press.

Blackburn, H. M. (2001). Dispersion and diffusion in coated tubes of arbitrary cross-section, *Computers and Chem. Eng.* **25**(2/3): 313–322.

Blackburn, H. M. (2002a). Mass and momemtum transport from a sphere in steady and oscillatory flows, *Phys. Fluids* **14**(11): 3997–4011.

Blackburn, H. M. (2002b). Three-dimensional instability and state selection in an oscillatory axisymmetric swirling flow, *Phys. Fluids* **14**(11): 3983–3996.

Blackburn, H. M. (2003). Computational bluff body fluid dynamics and aeroelasticity, *in* N. G. Barton and J. Periaux (eds), *Coupling of Fluids, Structures and Waves Problems in Aeronautics*, Notes in Numerical Fluid Mechanics, Springer, pp. 10–23.

Blackburn, H. M., Barkley, D. and Sherwin, S. J. (2008). Convective instability and transient growth in flow over a backward-facing step, *J. Fluid Mech.* **603**: 271–304.

Blackburn, H. M., Govardhan, R. N. and Williamson, C. H. K. (2000). A complementary numerical and physical investigation of vortex-induced vibration, *J. Fluids & Struct.* **15**(3/4): 481–488.

Blackburn, H. M. and Henderson, R. D. (1996). Lock-in behaviour in simulated vortex-induced vibration, *Exptl Thermal & Fluid Sci.* **12**(2): 184–189.

Blackburn, H. M. and Henderson, R. D. (1999). A study of two-dimensional flow past an oscillating cylinder, *J. Fluid Mech.* **385**: 255–286.

Blackburn, H. M. and Lopez, J. M. (2003a). On three-dimensional quasi-periodic Floquet instabilities of two-dimensional bluff body wakes, *Phys. Fluids* **15**(8): L57–60.

Blackburn, H. M. and Lopez, J. M. (2003b). The onset of three-dimensional standing and modulated travelling waves in a periodically driven cavity flow, *J. Fluid Mech.* **497**: 289–317.

Blackburn, H. M., Marques, F. and Lopez, J. M. (2005). Symmetry breaking of two-dimensional time-periodic wakes, *J. Fluid Mech.* **522**: 395–411.

Blackburn, H. M. and Schmidt, S. (2003). Spectral element filtering techniques for large eddy simulation with dynamic estimation, *J. Comput. Phys.* **186**(2): 610–629.

Blackburn, H. M. and Sherwin, S. J. (2004). Formulation of a Galerkin spectral element–Fourier method for three-dimensional incompressible flows in cylindrical geometries, *J. Comput. Phys.* **197**(2): 759–778.

Blackburn, H. M. and Sherwin, S. J. (2007). Instability modes and transition of pulsatile stenotic flow: Pulse-period dependence, *J. Fluid Mech.* **573**: 57–88.

Canuto, C., Hussaini, M. Y., Quarteroni, A. and Zang, T. A. (1988). *Spectral Methods in Fluid Dynamics*, Springer, Berlin.

Canuto, C., Hussaini, M. Y., Quarteroni, A. and Zang, T. A. (2006). *Spectral Methods: Fundamentals in Single Domains*, Springer.

Canuto, C., Hussaini, M. Y., Quarteroni, A. and Zang, T. A. (2007). *Spectral Methods: Evolution to Complex Geometries and Applications in Fluid Dynamics*, Springer.

Chin, C., Ng, H. C. N., Blackburn, H. M., Monty, J. and Ooi, A. S. H. (2015). Turbulent pipe flow at $Re_\tau = 1000$: a comparison of wall-resolved large-eddy simulation, direct numerical simulation and hot-wire experiment, *Computers and Fluids* . to appear.

Deville, M. O., Fischer, P. F. and Mund, E. H. (2002). *High-Order Methods for Incompressible Fluid Flow*, Cambridge University Press.

Dong, S., Karniadakis, G. E. and Chryssostomidis, C. (2014). A robust and accurate outflow boundary condition for incompressible flow simulations on severely-truncated unbounded domains, *J. Comput. Phys.* **261**: 83–105.

Elston, J. R., Blackburn, H. M. and Sheridan, J. (2006). The primary and secondary instabilities of flow generated by an oscillating circular cylinder, *J. Fluid Mech.* **550**: 359–389.

Funaro, D. (1997). *Spectral Elements for Transport-Dominated Equations*, Vol. 1 of *Lecture Notes in Computational Science and Engineering*, Springer, Berlin.

Gottlieb, D. and Orszag, S. A. (1977). *Numerical Analysis of Spectral Methods: Theory and Applications*, SIAM.

Guermond, J. L., Minev, P. and Shen, J. (2006). An overview of projection methods for incompressible flows, *Comp. Meth. Appl. Mech. & Engng* **195**: 6011–6045.

Guermond, J. L. and Shen, J. (2003). Velocity-correction projection methods for incompressible flows, *SIAM J. Numer. Anal.* **41**(1): 112–134.

Henderson, R. D. (1999). Adaptive spectral element methods for turbulence and transition, *in* T. J. Barth and H. Deconinck (eds), *High-Order Methods for Computational Physics*, Springer, chapter 3, pp. 225–324.

Henderson, R. D. and Karniadakis, G. E. (1995). Unstructured spectral element methods for simulation of turbulent flows, *J. Comput. Phys.* **122**: 191–217.

Karniadakis, G. E. (1989). Spectral element simulations of laminar and turbulent flows in complex geometries, *Appl. Num. Math.* **6**: 85–105.

Karniadakis, G. E. (1990). Spectral element–Fourier methods for incompressible turbulent flows, *Comp. Meth. Appl. Mech. & Engng* **80**: 367–380.

Karniadakis, G. E. and Henderson, R. D. (1998). Spectral element methods for incompressible flows, *in* R. W. Johnson (ed.), *Handbook of Fluid Dynamics*, CRC Press, Boca Raton, chapter 29, pp. 29–1–29–41.

Karniadakis, G. E., Israeli, M. and Orszag, S. A. (1991). High-order splitting methods for the incompressible Navier–Stokes equations, *J. Comput. Phys.* **97**(2): 414–443.

Karniadakis, G. E. and Sherwin, S. J. (2005). *Spectral/hp Element Methods for Computational Fluid Dynamics*, 2nd edn, Oxford University Press.

Kim, J., Moin, P. and Moser, R. (1987). Turbulence statistics in fully developed channel flow at low Reynolds number, *J. Fluid Mech.* **177**: 133–166.

Kirby, R. M. and Sherwin, S. J. (2006). Stabilisation of spectral/hp element method through spectral vanishing viscosity: application to fluid mechanics modelling, *Comp. Meth. Appl. Mech. & Engng* **195**: 3128–3144.

Koal, K., Stiller, J. and Blackburn, H. M. (2012). Adapting the spectral vanishing viscosity method for large-eddy simulations in cylindrical configurations, *J. Comput. Phys.* **231**: 3389–3405.

Korczak, K. Z. and Patera, A. T. (1986). An isoparametric spectral element method for solution of the Navier–Stokes equations in complex geometry, *J. Comput. Phys.* **62**: 361–382.

Maday, Y., Kaber, S. M. O. and Tadmor, E. (1993). Legendre pseudospectral viscosity method for nonlinear conservation laws, *SIAM J. Num. Anal.* **30**: 321–342.

Maday, Y. and Patera, A. T. (1989). *Spectral Element Methods for the Incompressible Navier–Stokes Equations*, State-of-the-Art Surveys on Computational Mechanics, ASME, chapter 3, pp. 71–143.

Pasquetti, R. (2006). Spectral vanishing viscosity methods for large-eddy simulation of turbulent flows, *J. Sci. Comp.* **27**(1–3): 365–375.

Patera, A. T. (1984). A spectral element method for fluid dynamics: Laminar flow in a channel expansion, *J. Comput. Phys.* **54**: 468–488.

Piomelli, U. (1997). Large-eddy simulations: Where we stand, *in* C. Liu and Z. Liu (eds), *Advances in DNS/LES*, AFOSR, Louisiana, pp. 93–104.

Reynolds, W. C. and Hussain, A. K. M. F. (1972). The mechanics of an organized wave in turbulent shear flow. Part 3. Theoretical models and comparisons with experiments, *J. Fluid Mech.* **41**(2): 263–288.

Rudman, M. and Blackburn, H. M. (2006). Direct numerical simulation of turbulent non-Newtonian flow using a spectral element method, *Appl. Math. Mod.* **30**(11): 1229–1248.

Sherwin, S. J. and Blackburn, H. M. (2005). Three-dimensional instabilities and transition of steady and pulsatile flows in an axisymmetric stenotic tube, *J. Fluid Mech.* **533**: 297–327.

Tadmor, E. (1989). Convergence of spectral methods for nonlinear conservation laws, *SIAM J. Num. Anal.* **26**(1): 30–44.

Xu, C. and Pasquetti, R. (2004). Stabilized spectral element computations of high Reynolds number incompressible flows, *J. Comput. Phys.* **196**: 680–704.

Zang, T. A. (1991). On the rotation and skew-symmetric forms for incompressible flow simulations, *Appl. Num. Math.* **7**: 27–40.